3-2002

Verification of MM5 Cloud Microphysics Schemes for East Asia

Dean J. Carter

VERIFICATION OF MM5 CLOUD MICROPHYSICS SCHEMES FOR EAST ASIA

THESIS

Dean J. Carter, Captain, USAF

AFIT/GM/ENP/02M-01

DEPARTMENT OF THE AIR FORCE
AIR UNIVERSITY

AIR FORCE INSTITUTE OF TECHNOLOGY

Wright-Patterson Air Force Base, Ohio

Report Documentation Page

Report Date	Report Type	Dates Covered (from... to)
14 Jan 02	Final	Sep 2000 - Jan 2002

Title and Subtitle Verification of MM5 Cloud Microphysics Schemes for East Asia	**Contract Number**
	Grant Number
	Program Element Number
Author(s) Captain Dean J. Carter, USAF	**Project Number**
	Task Number
	Work Unit Number
Performing Organization Name(s) and Address(es) Air Force Institute of Technology Graduate School of Engineering and Management (AFIT/EN) 2950 P Street, Bldg 640 WPAFB OH 45433-7765	**Performing Organization Report Number** AFIT/GM/ENP/02M-01
Sponsoring/Monitoring Agency Name(s) and Address(es) PACAF/DOWO ATTN: Mr. John Feckter 25 E St., Ste I232 Hickam AFB, HI 96853 AFWA/DNXM 106 Peacekeeper Dr. OFFutt AFB NE 68113-4039	**Sponsor/Monitor's Acronym(s)**
	Sponsor/Monitor's Report Number(s)

Distribution/Availability Statement
Approved for public release, distribution unlimited

Supplementary Notes
The original document contains color images.

Abstract
This research compares biases of the Reisner Mixed-Phase Explicit Moisture Microphysics graupel and non-graupel schemes to determine if including graupel and riming processes within the Fifth Generation Mesoscale Model (MM5) will lead to improved forecasts of winter precipitation for Korea and Japan. MM5 forecasts were generated every 12 hours for a 20-day case period from January 1998. Model derived meteorological fields were interpolated to the station coordinates of four verification sites within the East Asian domain and radiosonde observations were used to compare the differences between the average temperature and water vapor errors of the two cloud microphysics schemes. Analysis of the results shows significant differences between the schemes in the magnitude of humidity errors within the lower atmosphere of the model and provides evidence that the more complicated graupel and riming scheme will not increase the skill of the MM5 in forecasting winter precipitation for Japan and Korea. The underlying conclusion of this research is that AFWA should not alter the cloud microphysics scheme currently employed to determine winter precipitation type for its East Asian forecast window.

Subject Terms : Winter Precipitation, Fifth-Generation Mesoscale Model (MM5), Reisner Mixed-Phase Microphysics, Graupel and Riming Processes	
Report Classification unclassified	**Classification of this page** unclassified
Classification of Abstract unclassified	**Limitation of Abstract** UU
Number of Pages 88	

The views expressed in this thesis are those of the author and do not reflect the official policy or position of the United States Air Force, Department of Defense, or the U.S. Government.

AFIT/GM/ENP/02M-01

VERIFICATION OF MM5 CLOUD MICROPHYSICS SCHEMES FOR EAST ASIA

THESIS

Presented to the Faculty

Department of Engineering Physics

Graduate School of Engineering and Management

Air Force Institute of Technology

Air University

Air Education and Training Command

In Partial Fulfillment of the Requirements for the

Degree of Master of Science in Meteorology

Dean J. Carter, B.S.

Captain, USAF

March 2002

AFIT/GM/ENP/02M-01

VERIFICATION OF MM5 CLOUD MICROPHYSICS SCHEMES FOR EAST ASIA

Dean J. Carter, B.S.

Captain, USAF

Approved:

Ronald P. Lowther Advisory Committee Chairman	Date
Michael K. Walters (Member) Advisory Committee Member	Date
Daniel E. Reynolds (Member) Advisory Committee Member	Date

Acknowledgements

I would like to express my sincere gratitude to the many people who made this work possible. First, I want to thank my thesis advisor, Lt Col Ronald Lowther, not only for his technical assistance in preparing this document, but also for his personal mentorship during my time at AFIT. Additionally, I want to thank the other members of my committee: Lt Col Michael Walters for the expertise he provided in the field of numerical weather prediction and Professor Daniel Reynolds for his valuable help in the most challenging aspect of this research, the methods of statistical verification. I have a particular indebtedness to a fellow student, Capt William "Wild Bill" Courtemanche, who first showed me how to run the MM5 and, who better than anyone else, constantly challenged my research assumptions and offered me endless hours of vigorous debate. Finally, my greatest gratitude goes to my loving wife who has always been the rock to which I'm anchored. She was patient and understanding during my long "mental" absences from our family life and she gave me the strength and motivation to press on during the many difficult trials of this challenging program here at AFIT.

Dean J. Carter

Table of Contents

List of Figures

List of Tables

Abstract

This research compares biases of the Reisner Mixed-Phase Explicit Moisture Microphysics graupel (Option 7) and non-graupel schemes (Option 5) to determine if including graupel and riming processes within the Fifth Generation Mesoscale Model (MM5) will lead to improved forecasts of winter precipitation over Korea and Japan. The main purpose of this research was to make a recommendation to Air Force Weather Agency (AFWA) as to whether a more computationally expensive scheme is better suited for the East Asian theater. The ultimate goal is to find a way to reduce the negative impact winter precipitation places on military operations and public safety.

To explore the biases of these two Reisner schemes, MM5 forecasts were generated every 12 hours for a 20-day case period within January 1998. Gridded meteorological fields were interpolated to the station coordinates of four verification sites within the East Asian domain and radiosonde observations were used to compare the differences between the average temperature and water vapor errors of the two cloud microphysics schemes. Various scores were used to compare the success of the two Reisner schemes to categorically forecast precipitation type at the surface. Analysis of the results shows significant differences between the schemes in the magnitude of humidity errors within the lower atmosphere of the model and provides evidence that the more complicated Option 7 microphysics will not increase the skill of the MM5 to forecast winter precipitation for Japan and Korea. The underlying conclusion of this research is that AFWA should not alter the cloud microphysics scheme currently employed to determine winter precipitation type for its East Asian forecast window.

VERIFICATION OF MM5 CLOUD MICROPHYSICS SCHEMES FOR EAST ASIA

I. Introduction

1.1. Background of the Problem

The Chinese philosopher general Sun Tzu wrote the following words some 2,500 years ago: "If you know the enemy and know yourself, your victory will not stand in doubt; if you know Heaven and know Earth, you make your victory complete." By the word "Heaven", Sun Tzu meant the weather and its impact on warfare. This ancient truth is still very applicable today. Winter precipitation with its associated hazards impacts all aspects of military operations in any theater of warfare. Winter precipitation in the form of snow or ice storms can have disastrous consequences in terms of loss of life and destruction of property. In addition, both snow and freezing rain can have a significant impact on aircraft operations and the weapon systems employed by the United States Air Force (USAF).

Snowfall itself can create hazardous visibility conditions during the launch and recovery phases of aircraft operations. Freezing rain also has an extremely adverse impact on the performance of aircraft. USAF basing locations hit with a major snow or ice storm can expect at least a temporary loss of operational capability due to the need for snow or ice removal on runways, aircraft, roads, and equipment. Winter precipitation also has an adverse impact on offensive air operations. Freshly fallen snow has an average albedo of 0.8-0.9 (Barry and Chorley, 1968), which can affect the accuracy of

modern precision-guided munitions (PGMs). A ground-based target in a background of snowfall or ice cover will have a degraded infrared signature making it extremely difficult to image. With the air superiority enjoyed by the U.S. military in conflicts since World War II, our nation's enemies have used poor winter weather conditions to their advantage; for example, the 1950 winter offensive by Chinese forces during the Korean War. Proficient winter weather forecasting can minimize any advantage such as this to the enemy.

Yet, for USAF weather forecasters, forecasting winter precipitation is a very challenging endeavor. Since subtle environmental changes can result in different precipitation types, understanding and predicting winter precipitation in an operational environment proves both difficult and tasking; especially when considering the daily time constraints most operational forecasters are faced with. Therefore, USAF weather forecasters are placing ever-increasing reliance on numerical weather prediction (NWP) models for the forecasting of winter precipitation types. This research compares biases of two cloud and precipitation microphysics schemes of the USAF's primary operational NWP tool, the Fifth Generation Mesoscale Model (MM5), in forecasting winter precipitation types over Korea and Japan.

1.2. Statement of the Problem

Winter precipitation poses a negative impact to military operations, target acquisition, and public safety in general; therefore, reliance on the MM5 to accurately forecast winter precipitation will have adverse effects if biases within the model are not fully identified and understood by forecasters. Although MM5 is a fine grid-scale

numerical model, it requires a parameterization scheme to represent precipitation processes that occur on the sub-grid scale within the model. The MM5 used by the USAF utilizes the Reisner Mixed-Phase Explicit Moisture Microphysics option to handle these precipitation physics (MetEd, 2002). Biases within the Reisner mixed-phase scheme can be with the timing of the model, the MM5's thermal or moisture fields, or the vertical and horizontal resolution of these fields. An additional limitation of the Reisner mixed-phase scheme currently used is that it doesn't allow for riming and graupel processes within the atmosphere. Therefore, it's possible the model may misrepresent phenomena where these processes are important. However, the latest version of the Reisner scheme does account for riming and graupel processes.

The USAF utilizes several model windows for MM5 coverage of areas vital to the national interests of the United States. New windows are created as needed to focus on specific areas of interest (Operation Enduring Freedom for example). A worldwide verification study would be a difficult undertaking, therefore, it is necessary to focus on one theater of operations for feasibility reasons even though it is hoped the results will apply worldwide. Since the continental United States has been the main focus of most MM5 verification studies, East Asia is the focus of this particular research. Large numbers of U.S. military are stationed within this region, which experiences harsh winter weather conditions. This research particularly focuses on four locations: Osan Air Base (AB), South Korea; Kwang-Ju AB, South Korea; Misawa AB, Japan; and Wajima, Japan. The first three of the previously named locations are vital to the national security interests of the United States and are of great importance to U.S. Air Force operations in the region. Wajima was chosen to bring spatial balance to the sample data of the experiment

since research has shown the city lies within a region where graupel processes are known to be important mechanisms in the formation of winter precipitation (Hariyama and Sato, 1991). All four locations have widely different meteorological regimes that might cause the occurrence of winter precipitation types. Importantly, these locations all have 24-hour surface observing sites co-located with upper-atmospheric sounding sites and all have complete meteorological records spanning back many decades.

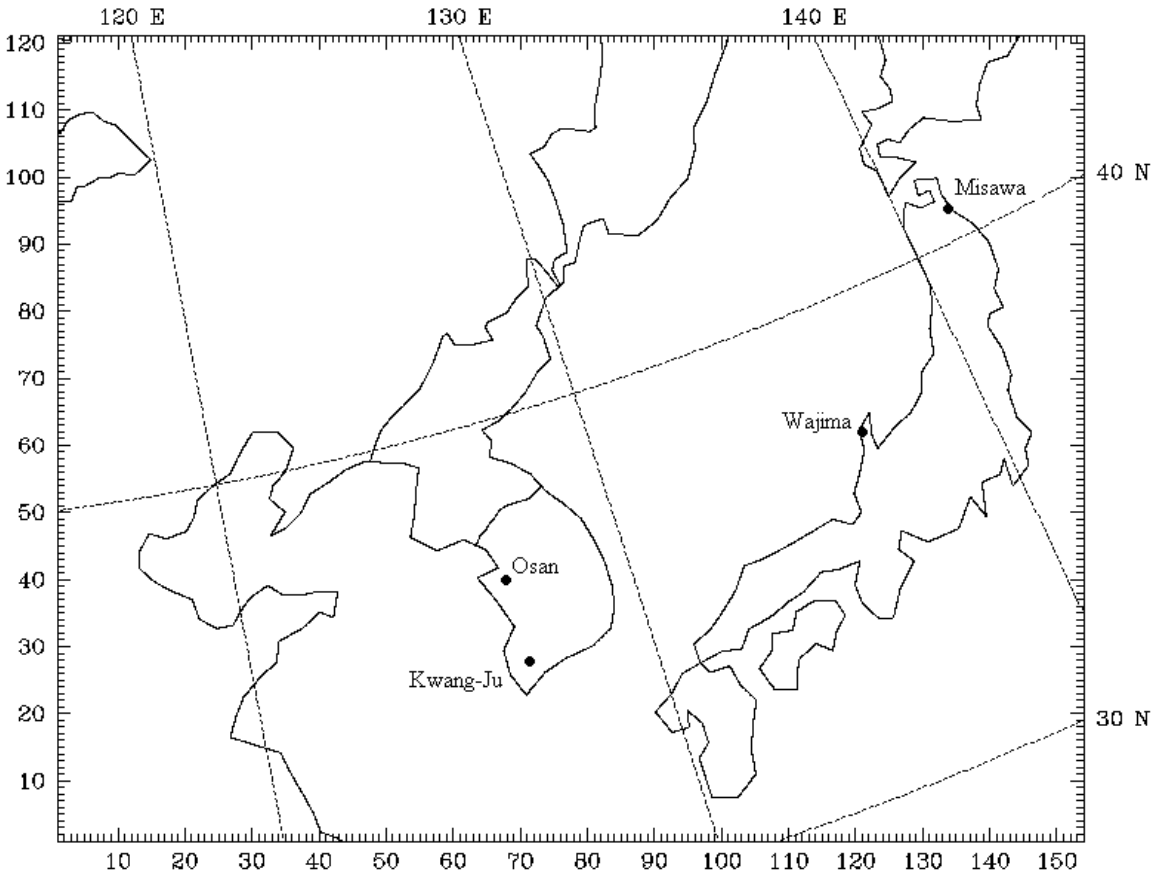

Figure 1. MM5 inner nest window used in the study. The map depicts locations used for forecast verification.

This research compares biases of two cloud microphysics schemes within the MM5 numerical weather prediction model used to forecast winter precipitation for these

sites in Korea and Japan. Comparing the Reisner mixed-phase no-graupel scheme with the latest Reisner graupel scheme shows if these riming and graupel processes significantly increase the MM5's skill to forecast winter precipitation for East Asia. Understanding any biases in MM5 winter precipitation schemes for the East Asian model window will improve prediction, increase weather warning lead times, and lessen the impact of winter precipitation on military operations in this highly critical theater. The results may also apply to MM5 windows worldwide in areas with similar winter weather regimes.

1.3. Research Objectives

The primary goal of this research is to examine biases in the MM5 numerical weather prediction model used in forecasting winter precipitation for the Korea and Japan by comparing two cloud microphysics schemes. The specific tasks necessary to achieve this goal are to:

1. Select a suitable case period to represent the winter weather regimes of Korea and Japan. Collect all observational weather data relevant to this study including temperature, humidity, and wind profiles from the surface throughout the upper troposphere. Perform a climatological data collection for Osan AB, Kwang-Ju AB, Misawa AB, and Wajima to provide a comprehensive database of winter precipitation events necessary for MM5 research.
2. Ingest observational data into and compile the MM5 model. This includes successfully setting up the East Asian domain window of the model to duplicate that used in forecasting by the USAF Weather Agency (AFWA) to include

duplicating all physical parameterizations used in AFWA's operational MM5 model.

3. Run the MM5 model twice over the East Asian domain for every 12 hours of the selected case period using the Air Force Institute of Technology's (AFIT) state-of-the-art meteorology lab. One run utilizes the Reisner non-graupel scheme, while the other uses the latest Reisner graupel scheme.
4. Statistically compare the MM5 output representing forecasts of vertical atmospheric profiles over the subject areas to archived observational upper-air soundings. In particular, dry-bulb temperature and mixing ratio profiles are compared in detail to determine average model bias. Liquid mixing ratios from 0 to -15ºC give an indication of the supercooled liquid water (SLW) content of the atmosphere. In addition, the depth of any cold/warm layers is critical to the formation of winter precipitation. A thorough statistical analysis is evaluated to determine the performance of each scheme and prove if there are any significant differences in winter precipitation forecasts between the two schemes.
5. Present the results of this study in the form of a formal thesis recommendation addressed to AFWA and other DoD archives as to which cloud microphysics scheme is better suited to forecast winter precipitation over East Asia. If the more computationally expensive graupel scheme is desirable, recommend if the additional computing time required is worth the benefit of a more accurate MM5 forecast.

II. Background and Literature Review

2.1. Winter Precipitation Physical Mechanisms and Processes

In order to understand the different microphysics schemes the MM5 uses to predict moisture variables that are used to derive precipitation type, knowledge of the physical mechanisms and processes of precipitation is important. It is widely known that precipitation occurs through either the processes of collision and coalescence or ice crystal growth in the atmosphere.

2.1.1. Warm Cloud Processes. Collision and coalescence are the primary precipitation formation mechanisms of warm clouds. A warm cloud is defined as a cloud that lays entirely below the level of the 0°C isotherm (Wallace and Hobbs, 1977) that is comprised of a high liquid content favorable for collision and coalescence (Rogers and Yau, 1989). Collision and coalescence are not important in snow development, but they are known formation mechanisms for other types of winter precipitation (Bernstein, 2000). The process occurs in both cumuliform and stratiform type clouds although with generally different length and time scales (Rogers and Yau, 1989).

In warm clouds, cloud droplets grow by condensation in a supersaturated environment. However, condensation by itself is not adequate enough to form drops that will precipitate. Growth to drop size is accomplished by collision and coalescence. In a typical distribution of cloud droplets, some drops will be larger and have higher terminal fall speeds than others and these drops will fall and impact with smaller drops. Although not a totally efficient process, enough smaller drops are usually captured and coalesced by the larger drops. If the drops grow large enough and are able to survive the updrafts

and downdrafts of the cloud without breaking up, they fall out of the base of the cloud in the form of rain or drizzle (Wallace and Hobbs, 1977).

2.1.2. Cold Cloud Processes. A cold cloud is defined as a cloud that extends above the level of the 0°C isotherm (Wallace and Hobbs, 1977). There are two subtypes of cold clouds. A mixed cold cloud has both supercooled water droplets and ice crystals, and its formation mechanisms include collision and coalescence and ice crystal growth, while a glaciated cloud only contains ice (Wallace and Hobbs, 1977).

Droplets in a mixed cloud freeze into ice particles by homogeneous nucleation (no foreign particles) or by heterogeneous nucleation (Wallace and Hobbs, 1977). Heterogeneous nucleation is around a small particle known as a freezing nucleus. The odds of heterogeneous nucleation occurring increases as the size of the supercooled drop increases. In a cold cloud, ice crystals can form directly from the vapor phase if particles known as deposition nuclei are present (Wallace and Hobbs, 1977). Table 1 depicts how the concentration of supercooled water droplets and ice particles depends on the location of cloud layers in relation to the 0°C isotherm.

In warmer layers of mixed clouds (0 to -15ºC), the concentration of ice particles is lower than that observed at colder temperatures, which allows for a higher storage of supercooled water. At temperatures below -15ºC, the concentration of ice crystals in combination with lower vertical velocities (typically 0.01 to 0.1 m s^{-1}) often associated with winter storms lowers the supercooled water concentration (Reisner et al., 1997).

The formation of precipitation in cold clouds first begins with growth by deposition in supersaturated and supercooled environments. However, the growth of ice particles by deposition is not enough to produce precipitation. Riming and aggregation

Table 1. Concentration of supercooled water and ice particles within cold clouds. (adapted from COMET (1998)).

0° to -4°C	Entirely supercooled droplets
-4° to -10°C	Approximately 50% ice particles
-10° to -20°C	>95% ice particles

are the processes that accomplish growth to precipitation size. Riming occurs in mixed clouds when supercooled droplets collide with ice particles and freeze upon impact, thus increasing the mass of the ice. Riming is a process that depletes supercooled liquid cloud water (Reisner et al., 1997). When riming increases the size of the ice crystal such that the original shape is no longer discernable, the ice crystal is referred to as graupel. The extreme case of graupel formation is hailstones found in thunderstorms. Aggregation occurs when ice particles with differing terminal fall speeds collide with each other (Wallace and Hobbs, 1977). As the size of an ice crystal increases due to riming and aggregation, the chances of further growth increases. If the terminal fall speed of the enlarged ice crystal is large enough to overcome the updraft velocity of the cloud and the environment, the particle will precipitate (Wallace and Hobbs, 1977).

Most winter precipitation is produced by nimbostratus. The precipitation forms through the ice crystal process as outlined in Table 2. In the ice crystal process, layers of the nimbostratus cloud colder than -20°C produce the ice crystals that precipitate to warmer layers where snow and graupel form by depositional growth, riming, and aggregation. If nimbostratus persists over long enough periods with cloud tops temperatures around -15°C, winter precipitation is quite possible (Rogers and Yau, 1989).

Table 2. Temperature roles in precipitation development within nimbostratus clouds. (adapted from COMET (1998)).

T < -20°C	Primary supplier of ice crystals for precipitation development
-10° > T > -20°C	Layer of rapid diffusional/depositional growth
0° > T > -10°C	Riming/aggregation proceed more rapidly-precipitation falls

2.2. Types and Characteristics of Winter Precipitation

An accurate forecast of winter precipitation type is very sensitive to the vertical profiles of temperature and moisture. Small-scale differences of temperature and humidity can lead to drastic differences in precipitation type experienced. Therefore, MM5 temperature and humidity biases are factors in the model's ability to accurately resolve these temperature and moisture differences between layers.

2.2.1. Precipitation Type RAOB Predictors. There are several predictors established through statistical methods to determine precipitation types and characteristics from rawindsonde observations (RAOB) or upper-air soundings. The first predictor is the mean temperature of the layer from the surface to 1000 meters above ground level (AGL). Temperature in this layer is important for discriminating between liquid and frozen precipitation. The mean temperature of the 500-2500 meter AGL layer can help in identifying the chance for freezing precipitation to occur (Bocchieri, 1980). Another predictor of winter precipitation is the depth of the warm layer, if one exists. A warm layer is defined by a temperature profile on a thermodynamic diagram that is completely greater than the 0°C isotherm (Bocchieri, 1980). The larger the area of the warm layer, the greater the chance that frozen precipitation melts as it transverses through the layer.

Wet-bulb temperature is a very important predictor of precipitation type. Wet-bulb temperature is used to account for the evaporational cooling that happens when precipitation falls through unsaturated air (Bocchieri, 1980). If moisture is added to the environment by evaporation to the point of saturation, the resulting temperature is the wet-bulb temperature. The less humid a layer of the atmosphere is, the greater the effect of evaporation. Cooling associated with evaporation can reduce the degree spread between the actual temperature and wet-bulb temperature up until the point of saturation (Bocchieri, 1980). Evaporating cloud droplets and precipitation are always at the wet-bulb temperature. Riming of snowflakes will deplete cloud water content and increase evaporational cooling and the wet-bulb temperature within the subsaturated layer beneath the precipitating cloud. In slight contrast to the wet-bulb temperature is the dew point temperature, which is defined as the "temperature to which a parcel of air is cooled at constant pressure until the water is saturated with respect to a plane surface of liquid water" (Wallace and Hobbs, 1977).

Two other precipitation type predictors are also related to wet-bulb temperatures. The first is the depth of the cold layer at the surface, if such a layer exists, with respect to the wet-bulb temperature profile. The second related predictor is the area on a thermodynamic diagram the wet-bulb temperature profile makes with the 0°C isotherm (Bocchieri, 1980). In addition, the number and spacing of vertical levels of an NWP model will determine whether the model can adequately resolve features of the cold and warm layer depths (Reisner et al., 1997).

Two additional moisture variables important in forecasting winter precipitation types are vapor pressure and the mixing ratio. The liquid water saturation vapor pressure

(e_{sw}) is an equilibrium state over a plane surface of water. The equilibrium state is reached when the rate of evaporation of molecules from the water surface to the air is the same as the rate of condensation from the air to the water surface (Wallace and Hobbs, 1977). Similarly, ice saturation vapor pressure (e_{si}) is the pressure equilibrium of saturated air to a plane surface of ice. Variables e_{sw} and e_{si} are given by:

$$e_{sw} = 6.112 \exp\left[17.67 \left(\frac{T - T_0}{T - 29.65}\right)\right] \qquad (1)$$

$$e_{si} = 6.11 \exp\left(22.514 - \frac{6150}{T}\right) \qquad (2)$$

where T_0 is the freezing point in Kelvin (Reisner et al., 1997). Equivalently, the vapor pressure of a subsaturated air parcel (e_w and e_i) can be determined by substituting dew point in place of temperature in equations 1 and 2. Since the mixing ratio is the ratio of the hydrometer mass (this includes cloud water, rain, snow, and graupel) to 1 kg of dry air, a parcel of air at saturation pressure is also at its saturation mixing ratio for water vapor (q_{sv}) and ice (q_{si}) and these four variables are related by:

$$q_{sv} = \frac{0.622\ e_{sw}}{p - e_{sw}} \qquad (3) \qquad\qquad q_{si} = \frac{0.622\ e_{si}}{p - e_{si}} \qquad (4)$$

Similarly, unsaturated mixing ratios for vapor and ice (q_v and q_i) are computed by substituting e_w and e_i for e_{sw} and e_{si} in equations 3 and 4. The mixing ratio is usually expressed in units of grams per kilogram (g/kg).

2.2.2. Characteristics of Precipitation Types. Although not in the category of winter precipitation, it is necessary to discuss the characteristics of rain and drizzle in order to distinguish these types from other forms of precipitation. A general way to

distinguish between rain and drizzle is that rain is comprised of drops greater than 200 μm in diameter (Stewart, 1985). Rain occurs at the surface whenever the surface warm layer is deep enough to melt all the snow (or occasionally ice pellets) before they reach the ground (Stewart, 1985). Because latent heat is released as snowflakes melt, there is usually an isothermal layer around 0°C when precipitation is happening (Stewart, 1985). Studies of sounding profiles and radar "bright bands" indicate the melting layer can be several hundred meters thick (Rogers and Yau, 1989).

The typical vertical temperature profile for snow is colder than 0°C throughout the lower troposphere. The probability of snow is not dependent on the slope of the lapse rate, but only on temperatures being less than freezing within the snow producing cloud. Snowflake size is also temperature dependent, with larger snowflakes more typical at temperatures near 0°C. This is due to the increased aggregation of snowflakes, which is at its highest efficiency near freezing (Stewart, 1985). Although produced at temperatures less than freezing, falling snow can exist at temperatures above freezing because the precipitation does not immediately totally evaporate or melt into rain.

Mixed precipitation usually involves the presence of both rain and snow at the surface. The 0°C isothermal layer is closer to the surface than what would be experienced in a strictly rain event. This isothermal layer is usually on the order of 1 km deep. Snowflakes that fall in a mixed precipitation event are usually large since aggregation conditions are ideal. A mixed precipitation event can rapidly turn into a strictly snow event if evaporation of falling precipitation within the subsaturated layer beneath the precipitating cloud extends the freezing level down to the surface.

Freezing rain occurs when snow or ice pellets melt completely into supercooled droplets while falling through an inversion layer aloft before falling into a sub-zero layer near the ground level (Zerr, 1997). There is insufficient time for the raindrops to refreeze before impacting the surface. Freezing rain and freezing drizzle are considered more destructive than snow because the freezing precipitation coats exposed surfaces, including aircraft, in a glaze of ice. The warm layer aloft is on the order of 1 km deep, while the thickness of the surface subfreezing layer is also around 1 km. Studies have shown that if a near surface layer is close to saturation and the ground is freezing, a 1000-850 mb thickness value less than approximately 1314 meters and a 850-700 mb thickness value greater than approximately 1539 meters may indicate a possible freezing rain event (Stewart, 1985). Studies have shown that cold air advection at the surface and warm air advection aloft (known as overrunning) is typically responsible for a typical freezing rain scenario (Zerr, 1997).

The actual temperature profile between freezing rain and freezing drizzle events can be quite different. Temperatures at the surface are usually colder in a freezing drizzle event and the saturated layer is usually shallower. Studies have also shown that sizable minorities of freezing drizzle events don't even have any warm layer above sub-freezing layer. When this occurs, collision and coalescence of supercooled droplets is thought to be the main mechanism for freezing drizzle formation (Bocchieri, 1980).

Similar to freezing rain, ice pellets occur when snow melts completely while falling through an inversion aloft before falling into a sub-zero layer near the ground level (Stewart, 1985). However, as opposed to freezing rain, there is sufficient time for the raindrops to refreeze before impacting the surface. Ice pellets are sometimes referred

to as sleet in North America and are described as small balls of smoothly glazed ice. Most ice pellets have a frozen center, although some have been observed having liquid centers. This suggests that refreezing of the drop occurs from the surface inwards (Wallace and Hobbs, 1977). Compared to freezing rain, ice pellet events occur with lower values of surface temperatures and thicker refreezing layer depths (Zerr, 1997). Similar to freezing rain, cold air advection at the surface and warm air advection aloft are present during an ice pellet event (Zerr, 1997).

As discussed previously, accurate forecasts of winter precipitation types are very sensitive to vertical profiles of temperature and moisture. Small-scale differences in these model derived variables can mean drastic differences in the precipitation type predicted. MM5 temperature and humidity biases are factors in the model's ability to accurately resolve these temperature and moisture differences between layers. Inaccurately predicted temperature and humidity variables will contribute to incorrect forecasts of surface precipitation type in the MM5 post-process.

2.3. General Description of the MM5

The MM5 is a mesoscale finite difference (centered in time and space) model that works on a nonhydrostatic assumption due to the fact that the atmospheric motions the model represents are too small for the hydrostatic assumption to be valid (Grell et al., 1994). The model allows for 4-dimensional data assimilation from radiosonde observations (RAOBs), surface observations, ship and buoy reports, and data from other numerical weather prediction models such as the Aviation (AVN) and Eta.

2.3.1. MM5 Horizontal Grid. The MM5 can handle multi-nested windows each having a staggered grid. In particular, the model utilizes the Arakawa B-grid (Grell et al., 1994). A depiction of the Arakawa B-grid is shown in Figure 2. The model represents the horizontal wind field at the grid locations where the dots are. Scalar quantities such as the 3-D temperature, mixing ratios (water vapor, cloud water, cloud ice, etc.) and vertical velocities are represented at the cross points (Grell et al., 1994).

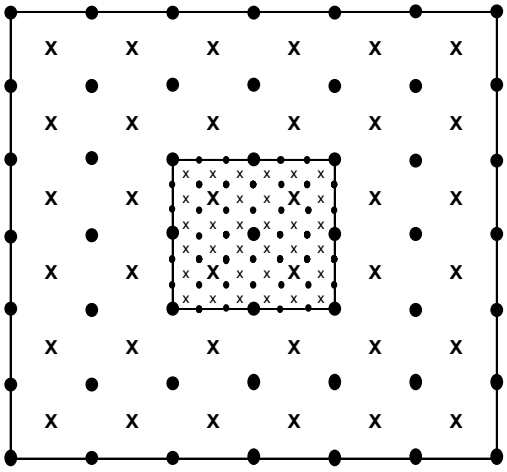

Figure 2. Horizontal Arakawa B-grid used in the MM5 (adapted from Dudhia (2001)).

2.3.2. Sigma Levels. The vertical coordinates for the MM5 are known as sigma levels. Sigma levels redefine the vertical height coordinates to a variable that simplifies the model's equations (Grell et al., 1994). The MM5's sigma levels are based on pressure at the surface and top layer of the model:

$$\sigma = (p - p_t)/(p_s - p_t) \qquad (5)$$

where p is pressure, p_s is pressure at the surface, and p_t is pressure at the top layer of the model. Sigma levels have the advantage that they follow the terrain of the model (Grell et al., 1994). In the MM5, the only variable defined at each sigma level is vertical velocity. Cross point scalar variables such as temperature and mixing ratio are defined at half-sigma levels. A much more detailed description of the MM5 is provided in Grell et al. (1994).

2.4. Parameterization Schemes

The processes of NWP models occur on two scales, the grid scale and sub-grid scale. Grid scale dynamics include momentum, advection, vorticity, and divergence. Although the MM5 is considered a "fine scale" model, it cannot resolve sub-grid atmospheric processes (with typical 45 or 15 km^2 grids) with the finite difference method (COMET, 1998). Examples of these processes are heat and moisture fluxes, planetary boundary layer (PBL) processes, cumuliform cloud formation, and the subject of this research -- precipitation physics. Therefore, the model uses parameterization schemes to represent these physical phenomena. Parameterization schemes interact with grid scale processes and with each other (COMET, 1998).

2.4.1. Cloud/Precipitation Parameterization. Both Reisner schemes are explicit in that they account for resolved precipitation physics (Grell et al., 1994). Both schemes are activated whenever grid-scale saturation is reached. The cross points represent the average conditions of the grid boxes; and the only moisture variable present at the time of model initialization is water vapor. All other moisture variables receive a "cold start" in that they are not generated until the grid box reaches a critical value below complete

saturation when both schemes start to create cloud water and ice. Whenever water vapor condenses into liquid or sublimates into ice, latent heat is released thus warming the environment. As precipitation falls within the cloud, however, cloud temperatures drop and humidity increases as a result of evaporational cooling. As precipitation falls from

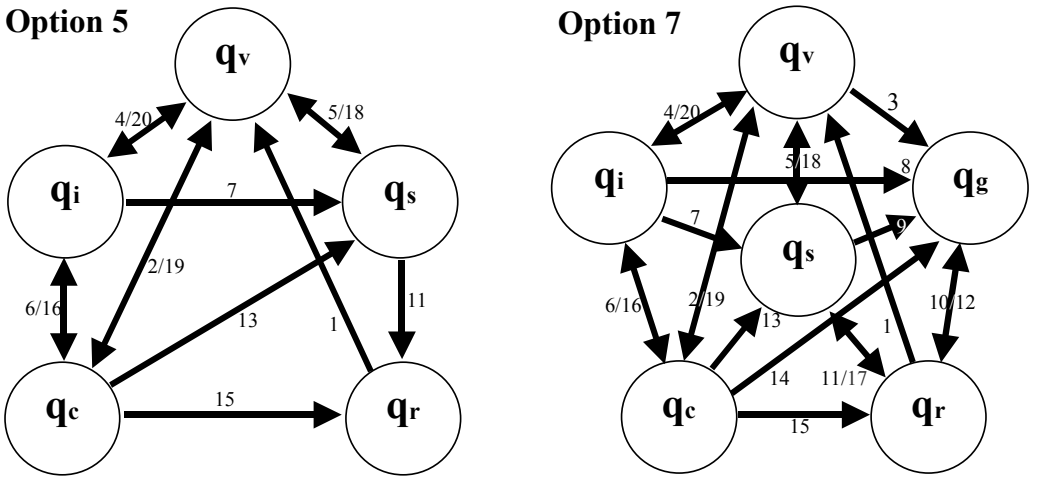

Key

1. Reduction of rain by evaporation
2. Generation of cloud water by condensation
3. Generation of graupel by deposition
4. Generation of ice by deposition or nucleation
5. Generation of snow by deposition
6. Generation of cloud water by melting
7. Generation of snow by conversion or collection
8. Generation of graupel by collection or collision of
9. Generation of graupel by collection or collision of
10. Generation of rain by melting graupel
11. Generation of rain by melting snow
12. Generation of graupel by collection or freezing of
13. Generation of snow by accretion
14. Generation of graupel by accretion or collection
15. Generation of rain by conversion or collection
16. Generation of ice by freezing or collection
17. Generation of snow by accretion of rain
18. Sublimation of snow
19. Evaporation of cloud
20. Sublimation of ice

Figure 3. Reisner mixed phase parameterization schemes (adapted from Grell et al. (1994) and Reisner et al. (1997)).

the cloud, the subsaturated layer cools and moistens (COMET, 1998). The Reisner schemes track precipitation as it falls (Reisner et al., 1997), resulting in a more realistic evaporational cooling rate compared to schemes that have precipitation falling immediately to the ground.

2.4.2. Reisner Mixed-Phase, Non-Graupel Scheme. The Reisner Mixed-Phase Scheme (Option 5 on the list of MM5 explicit moisture schemes) currently employed by AFWA has an advantage over implicit cloud/precipitation microphysics schemes in that it allows for the presence of supercooled water and ice crystals within the same vertical layer. Supercooled liquid water is generated in response to the MM5's vertical motion fields (Reisner et al., 1997). Another advantage is that snow can exist at temperatures above freezing. Option 5 carries variables for mixing ratios of water vapor (q_v), cloud water (q_c), cloud ice (q_i), snow (q_s), and rain (q_r). The interaction of these mixing ratios is depicted in Figure 3. In Option 5, ice crystal concentrations are not directly predicted, but are prescribed by use of curves first specified by Fletcher (1962):

$$n_i = n_0 \exp [\beta(T_0 - T)] \qquad (6)$$

In the "Fletcher Curve" n_i is the ice nucleus concentration, T is temperature (K), n_0 is a constant (10^{-2} m^{-3}), β is a constant (0.6 K^{-1}), and T_0 is the freezing level temperature (Rutledge and Hobbs, 1984). However, the number concentrations for rain and snow are directly predicted in Option 5 (Grell et al., 1994).

It is important to note that the MM5 does not directly forecast surface precipitation types; rather, these are derived from the model predicted mixing ratios shown in Figure 3. Rain, snow, and graupel that are generated at a model sigma level will fall to the next sigma level. Falling between sigma levels, the precipitation will undergo evaporation, which will change the mixing ratio of the hydrometer. It is this change in mixing ratio between sigma levels that is used to predict precipitation type (MetEd, 2002). The first step of the post model run diagnosis of snowfall using the

Option 5 predicted q_s fields is to calculate the slope intercept of the snow concentration, which is given by:

$$N_{0s} = \left[1.718 \left[\frac{6\ \rho_w}{\rho_d\ a_s\ \Gamma\left(4 + b_s\right)} \left(\frac{\pi\ \rho_s}{\rho\ q_s} \right)^{\frac{b_s}{4}} \right]^{0.94} \right]^{\frac{4}{4 - 0.94\ b_s}} \qquad (7)$$

In the above equation, a_s and b_s are snowfall speed constants, ρ_d is the dry air density, ρ_s is the density constant for snow (100 kg m^{-3}), ρ_w is the density constant for water (1000 kg m^{-3}), and Γ is the gamma function. As the snow mixing ratio approaches zero, N_0 approaches infinity. Therefore, the scheme sets an upper limit for N_0 of 2 x 10^7 m^{-4} (Reisner et al., 1997). The next step in snowfall determination is calculation of the slope parameter for the snow distribution given by Rutledge and Hobbs (1984):

$$\lambda_s = \left(\frac{\pi\ N_{0s}\ \rho_s}{\rho_d\ q_s} \right)^{0.25} \qquad (8)$$

From this, it is possible to determine the mass-weighted snowfall speed, which is given by Reisner et al. (1997) as:

$$V_{sf} = a_s \frac{\Gamma\left(4 + b_s\right)}{6} \lambda_s^{-b_s} \qquad (9)$$

Due to the effects of evaporation, precipitation of snow will change the snow mixing ratio according to:

$$\text{Precip}_{(\text{snow})} = -\frac{\partial}{\partial \sigma} V_{sf}\ \rho_d\ g\ q_s \qquad (10)$$

where g is the gravitational acceleration (Reisner et al., 1997). If the fall rate for the snow mixing ratio at the surface is at least 2 x 10^{-7} g/kg per sigma level, snowfall is diagnosed at the surface (MetEd, 2002).

2.4.3. Reisner Mixed-Phase Graupel Scheme. The Reisner Mixed-Phase Graupel Scheme (Option 7 on the list of MM5 explicit moisture schemes) is based on Option 5. However, the major difference between the two schemes is the inclusion of a mixing ratio variable for graupel (q_g). The scheme produces snow by accretion of cloud water, conversion of ice into snow, collection of ice by snow, and generation by depositional growth. Option 7 introduces riming as processes in the growth of cloud ice, which directly influences snow production. Riming depletes cloud water faster, causing evaporational cooling of the environment and an increase in wet-bulb temperature, which are conditions that will prevent snow from otherwise melting (Reisner et al., 1997).

Option 7 also uses the Fletcher Curve for ice crystal initiation. However, in order to limit the ice particle concentration at cold temperatures, a minimum limit of -27ºC is set (Resiner et al., 1997). There is also a number concentration bound such that the scheme will not generate large numbers of ice particles at small values of q_v. The determination of snowfall is the same as that used with the Option 5 q_s fields. Although, the methods of snowfall determination are the same, snow mixing ratios will differ between the two schemes due to the presence of graupel since the two hydrometers

compete for the same supercooled liquid water. Analysis of the Fortran code of Option 7 reveals that the slope intercept of graupel concentration is given by:

$$N_{0g} = 2.38 \left(\frac{\pi \rho_g}{\rho_d q_g} \right)^{0.92} \qquad (11)$$

where ρ_g is the density constant for graupel (400 kg m^{-3}). The slope parameter distribution can then be given by:

$$\lambda_g = \left(\frac{\pi N_{0g} \rho_g}{\rho_d q_g} \right)^{0.25} \qquad (12)$$

which, in turn, is used to calculate the fall speed of the graupel:

$$V_{gf} = a_g \frac{\Gamma(4 + b_g)}{6} \lambda_g^{-b_g} \qquad (13)$$

In the above equation, a_g and b_g are constants in the fall speed relationship for graupel which have values of 19.3 and 0.37 respectively (Reisner et al., 1997). Similar to snow, the precipitation of graupel will change the graupel mixing ratio according to:

$$\text{Precip}_{(gr)} = -\frac{\partial}{\partial \sigma} V_{gf} \rho_d g q_g \qquad (14)$$

There are two ways Option 7 q_s fields will lead to diagnosis of snow at ground level. The first, similar to that described for Option 5 q_s fields, occurs when the fall rate for the snow mixing ratio at the surface is at least 2 x 10^{-7} g/kg per sigma level. The second prediction of snow occurs if the fall rate for the graupel mixing ratio at ground

level is greater than 1 x 10^{-6} g/kg per sigma level, the surface ambient temperature is between 0 and 2ºC, and the maximum rain mixing ratio at any level in the subsaturated air column is less than 0.05 g/kg or the graupel fall rate at the surface level is less than that for snow (Carbin, 1999).

The prediction of freezing rain at the surface is the same as that for rain except the surface temperature is below freezing and the fall rate for the rain mixing ratio at ground level is greater than 10 g/kg per sigma level. The prediction of ice pellets is related to the graupel processes of Option 7. A diagnosis of ice pellets at ground level happens when the q_g fall rate at that level is greater than 1 x 10^{-6} g/kg per sigma level, the surface ambient temperature is less than freezing, the maximum rain q_r at any level in the subsaturated air column is less than 0.05 g/kg, and the q_g fall rate is greater than the q_s fall rate (Carbin, 1999).

2.5. Previous MM5 Winter Precipitation Verification Studies

A literature review has found several previous verification studies that sought to expose biases in the MM5's ability to forecast winter precipitation. All of these studies focused on the continental United States and used varying cloud and precipitation microphysics schemes of increasing complexity. The results of two studies that dealt with mixed-phase microphysics are briefly discussed here.

Manning and Davis (1997) performed a statistical verification study of MM5 using satellite and RAOB data collected during the Winter Icing and Storms Project of 1994 (WISP94). WISP was an on-going project "designed to further our understanding of the dynamical and microphysical processes leading to the production and depletion of

supercooled liquid water in winter storms and to improve forecasts of aircraft icing" (Rasmussen et al., 1992). WISP94 focused on the initiation of ice crystals and the scope of the project covered the entire Western U.S. (Manning and Davis, 1997).

Manning and Davis (1997) ran a non-hydrostatic MM5 with 27 sigma levels. There were three domains at 60, 20 and 6.7 km resolutions, and these grids were two-way nested. Forecasts were run out to 24 hours and utilized Option 5 for the cloud microphysics scheme.

In Manning and Davis verification study, radiosonde observations were compared to forecast MM5 soundings. Data from RAOBs were interpolated at 40-meter intervals to match the vertical output from the MM5 (Manning and Davis, 1997). Statistical comparisons between soundings and 12-hour and 24-hour MM5 forecasts were performed. Analysis revealed that at the 12-hour point, the MM5 had a warm bias (>2°C) in the upper levels of the atmosphere near the tropopause and a cold bias (≈ 0.75°C) in the lower levels. At the 24-hour point, the MM5 showed a cold bias of 0.5-1.0°C in the low levels (Manning and Davis, 1997).

This study also showed moisture biases. At 12 hours, the MM5 tended to over forecast mixing ratios from the surface to 800 mb and also between 600 and 300 mb. The moist bias at these levels increased to a maximum of 35% over prediction by 24 hours. The upper-level bias tended to occur where the model determined the level of maximum ice cloud. The bias statistics were found to be similar between the 60 and 20-km horizontal grids used in the project (Manning and Davis, 1997).

One hypothesis Manning and Davis put forth regarding the temperature and humidity biases found in the WISP94 MM5 verification study is that the MM5 is prone to

overforecast high cloud cover (Manning and Davis, 1997). As previously stated, Option 5 uses the Fletcher Curve to calculate ice particle concentration as a function of temperature. This tends to over predict cloud ice near the 400 to 300 mb levels. Option 5 will only deplete cloud ice by melting, sublimation, accretion, or conversion to snow. However, the 400 to 300 mb level is too cold for melting and since little snow is formed at these levels, the model maintains the ice in extensive cloud cover over the Western U.S. (Manning and Davis, 1997).

By causing reduced short-wave radiation, Manning and Davis (1997) believe this extensive cloud cover aloft contributes to the low-level cloud biases. The authors also hypothesize that this lack of short-wave radiation contributes to the MM5's inability to accurately model both daytime and nighttime boundary layers and nocturnal inversions. Another possible source of this low-level bias is the MM5's process of parameterizing available surface moisture data. The MM5 categorizes the moisture availability of terrain on a scale from 0.0 (completely dry) to 1.0 (over water). The model uses the moisture availability to calculate humidity on the surface and latent heat fluxes as well. The WISP94 verification study found the MM5 produced too cool and too moist boundary layers (Manning and Davis, 1997). This cold low-level bias could be a factor in non-representative forecasts of winter precipitation types, especially that of freezing rain and ice pellets.

Perhaps Reisner, Rasmussen, and Bruintjes (1997) performed the most thorough mixed-phase microphysics study for the MM5 in 1996. This study focused on the verification of the MM5's ability to forecast supercooled liquid water in winter storms compared to observations collected during the Winter Icing and Storms Project of 1990

(WISP90). The MM5 used in this previous research had 27 sigma levels and 60, 20, 6.7, and 2.2 km horizontal grids situated over the western United States. These grids were two-way nested for the 60 and 20 km domains, but the 6.7 and 2.2 domains were one-way nested.

The Reisner et al. study used three mixed-phase cloud and precipitation microphysics schemes of increasing complexity. The first option directly predicted the mixing ratios for cloud, rain, snow and ice. Snow and ice concentrations were prescribed. The second option added mixing ratio for graupel to the list of mixing ratios explicitly predicted in the first option and it also explicitly predicted the number concentration of ice particles. The third option was even more complex by including explicit prediction of snow and graupel number concentrations (Reisner et al., 1997). The third option used in the Reisner et al. study is the same as Option 7 of the AFWA MM5, but a scheme equivalent to Option 5 was not used.

The authors concluded the third scheme had the best performance in forecasting supercooled liquid water when compared to observed fields. However, the second option also performed well if the number concentration of snow was allowed to vary in accordance with snow mixing ratios. The authors also confirmed the importance of riming of snow and/or graupel in the depletion process of supercooled liquid water (Reisner et al., 1997).

III. Data Collection and Methods of Analysis

3.1. Data Sources

The Air Force Combat Climatology Center (AFCCC), located in Asheville, NC, provided archived observational data for use in this study. These data were provided in Microsoft Excel format for the purpose of data sorting. MM5 meteorological input files were provided by the National Center for Atmospheric Research (NCAR) from the National Center for Environmental Prediction (NCEP) Global Data Assimilation System (GDAS) database in GRIB (**Gri**dded **B**inary) format. These data sets are available from NCAR on a 12-hourly basis spanning back decades and are archived on a 2.5° by 2.5° latitude/longitude grid. The terrain data used as input into the MM5 were obtained from the U.S. Geological Survey (USGS).

3.2. Control Data

The control data for this experiment included archived RAOBs from all four locations. These archived weather balloon reports provide a detailed vertical profile of temperature and dew point with relation to height in the atmosphere. From these directly observed data, pressure and winds are inferred (pressure as a result of the hydrostatic approximation). As a minimum, each RAOB reports at what are termed as mandatory levels. These are the temperature, dew point, and winds at the surface, 1000, 925, 850, 700, 500, 400, 300, 200, 150, and 100 mb levels. In addition to these mandatory levels, significant levels are also reported. A level is deemed significant if the observed

temperature lapse rate deviates from average lapse rate for dry and moist air respectively or there are abrupt changes in moisture at that level. Since the accuracy of humidity measurements at higher altitudes are highly suspect (Manning and Davis, 1997), mixing ratio observations above the 500 mb level were discarded. In addition, balloon drift and its associated spatial errors were ignored.

For the purpose of this research, RAOBs spanning a continuous 20-day period within January 1998 were used. The reporting time for these observations were 0000 and 1200 Greenwich Mean Time (Z) which corresponds to 0900 and 2100 Local Standard Time (L) in Korea and Japan. A database of surface observations was used to determine occurrences of winter precipitation during the 20-day period of study. Additional data provided by AFCCC gave information on daily snowfall amounts. A detailed background of the geography of the verification sites along with the synoptic regimes that produced winter precipitation during the period of study is provided in Appendix A.

3.3. Method of Analysis

To explore biases in the two Reisner options in forecasting winter precipitation for East Asia, two MM5 forecast model runs were required every 12 hours for the entire 20-day study period. In particular, the process of data collection entailed:

1) Acquiring GDAS datasets, RAOBs, and surface observations for the period of study.
2) Running the MM5 initialized at 00Z and 12Z for each day of the case period simultaneously using Option 5 and Option 7 microphysics.

3) Converting the MM5 binary output to an alphanumeric format and employing a weighted-average scheme to interpolate gridded meteorological fields to the actual station locations of Osan, Kwang-Ju, Misawa, and Wajima.
4) Exporting the above output to the software packages Excel, Mathsoft MATHCAD, and SAS Institute JMP for statistical analysis.

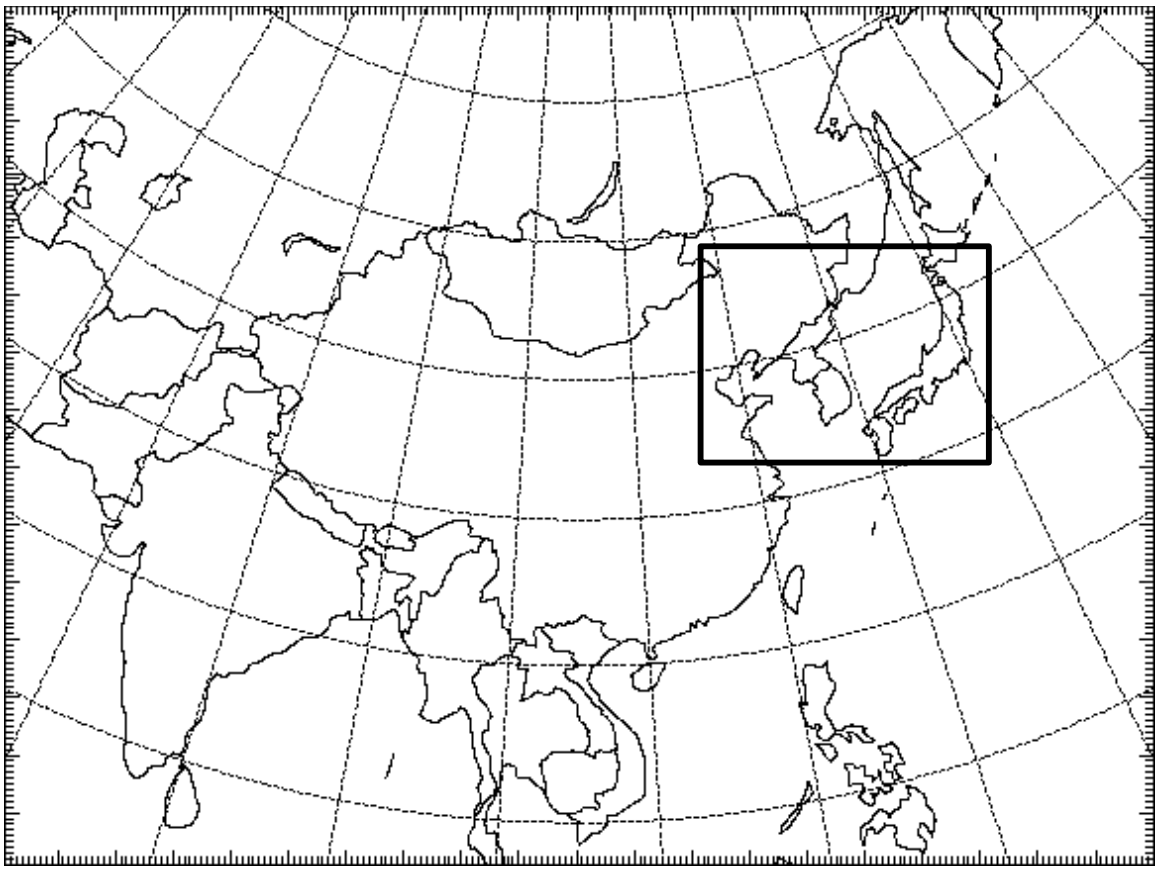

Figure 4. MM5 outer nest with overlay of inner nest.

3.3.1. MM5 Process. Two MM5 forecast windows situated over East Asia were used in this experiment. The first window, the outer nest, has a horizontal resolution of 45 km on a 200 by 150 grid and 41 vertical sigma levels. The inner nest has a horizontal

resolution of 15 km on a 154 by 121 grid with 41 sigma levels. These nests are duplicates of the T6A and T6B windows used by AFWA. Since running the inner nest simultaneously with the outer nest in a two-way nesting scheme proved too time consuming given the available computer resources at AFIT, the NESTDOWN procedure was used instead. NESTDOWN horizontally interpolated sigma coordinate data from the outer nest to the inner nest, providing the boundary conditions for the inner nest run. The use of NESTDOWN is further justified since AFWA currently uses the same technique. All files in the MM5 suite of programs are written in Fortran code.

Utilizing the program module TERRAIN was the first step of each MM5 numerical weather forecast. TERRAIN was used to horizontally interpolate latitude/longitude terrain elevation and vegetation and soil characteristics onto both outer and inner nest grids. TERRAIN output this information in files used in later MM5 modules. The resolution of the terrain elevations used in this study is 10 minutes (18.5 km) for the outer nest and 5 minutes (9.25 km) for the inner nest. Figure 5 shows the terrain map of the inner nest.

The next step of the MM5 model run was utilizing the program REGRID. The first portion of REGRID ingested archived gridded analyses on horizontal surface and upper pressure levels. The second portion interpolated these observations from the original grid and map projection to the outer nest grid and map projection defined by TERRAIN. The observational analyses used in this study were from the NCEP GDAS database. For its REGRID input, AFWA utilizes the NCEP Aviation (AVN) model.

The use of AVN means that AFWA doesn't use observations to initialize its MM5. Rather, AFWA uses a 6-hour AVN forecast that is assumed to be a good

representation of the initial conditions of the model run. AVN is a global spectral model that is only available in real time. For this reason, the use of AVN was not feasible for the purpose of this research. However, since previous MM5 verification studies generally have used GDAS for input, a premise of this research is that any statistical results using GDAS will also be applicable to a MM5 model utilizing AVN.

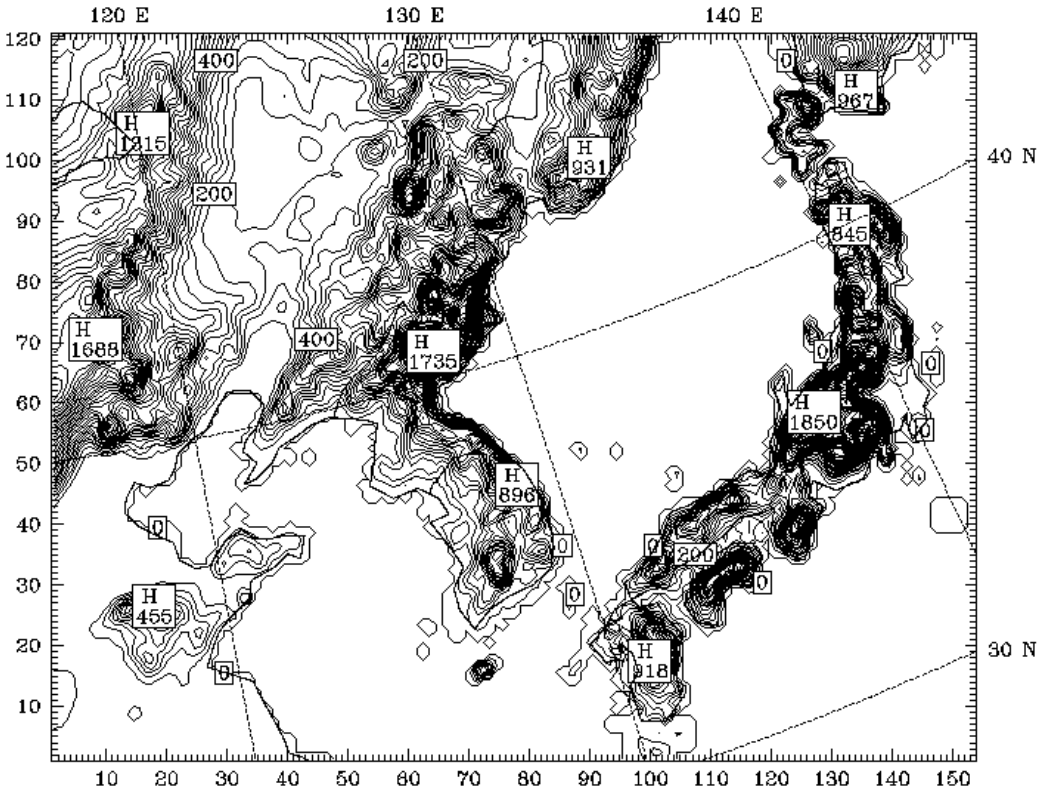

Figure 5. Terrain map of the MM5 inner nest used in this study. Elevations are contoured every 50 meters.

The output from REGRID was used in the module RAWINS. The purpose of RAWINS was to improve the coarse grid output of REGRID by ingesting RAOBS and surface observations that matched the outer nest domain and forecast time. According to the strength and curvature of the pressure level winds, RAWINS used the modified

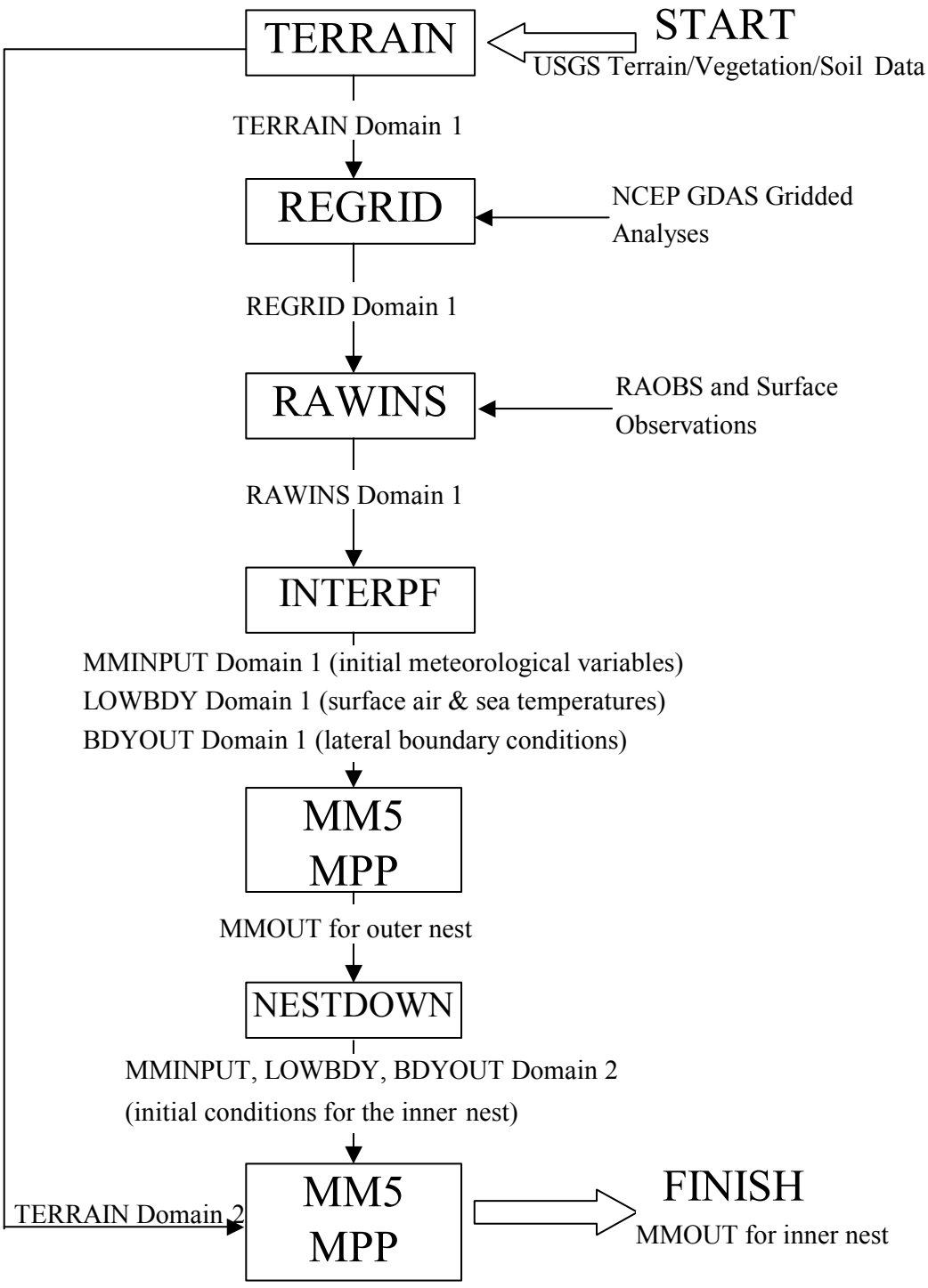

Figure 6. The MM5 forecast process.

Cressman Ellipse and Banana Schemes for its objective analysis (Grell et al., 1994). In this research, RAWINS was substituted for the Multivariate Optimum Interpolation (MVOI) scheme used by AFWA to assimilate observations into the coarse grid analysis. MVOI is used to make corrections to the 6-hour AVN forecast used by AFWA to initialize the MM5.

The next step of each MM5 run utilized the module INTERPF. The purpose of INTERPF was to provide the initial conditions for the lateral and lower boundaries of the outer nest window. In order to provide these initial conditions, INTERPF vertically interpolated from pressure coordinates to the MM5's sigma levels and then computed initial meteorological values such temperature and humidity.

With the necessary input files from TERRAIN and INTERPF accomplished, the actual numerical weather prediction part of the MM5 outer nest was run on multiple Unix processors out to 24 hours using a 100 second time step. In addition to the Option 5 and 7 cloud microphysics schemes, the MM5 model used in this research utilized the Grell Cumulus Parameterization Scheme for cumulus convection, the Medium Range Forecast (MRF) PBL Scheme to account for surface radiation, and the Cloud Radiation Scheme to depict solar and terrestrial radiation interaction with clouds and clear-air. To account for ground temperature, a five-layer soil model was used. Aside from the Option 7 microphysics, all parameterization schemes used in this research were the same as used currently by AFWA.

As mention previously, when the outer nest forecast was complete, its domain output was used by NESTDOWN to create input files for the higher resolution inner nest that was used in conjunction with the fine grid inner nest TERRAIN output. This method

is known as one-way nesting since there is no feedback from the inner nest to the outer nest that would occur with two-way nesting (Grell et al., 1994). With the modified initial, boundary, and lateral conditions, the second NWP portion of the MM5 ran the inner nest out to 24 hours at a 45 second time step.

3.3.2. MM5 Post-Processing. In order to view the final MM5 forecasts, a graphics program entitled RIP (which stands for Read/Interpolate/Plot) was utilized. RIP is designed to invoke NCAR graphics routines for the purpose of viewing MM5 output graphically (Stoelinga, 2000). In order to view forecast vertical soundings for Wajima, Misawa, Osan, and Kwang-Ju, the RIP station list was modified to account for these sites by including their World Meteorological Organization (WMO) number, latitude/longitude coordinates, and station elevations. With this information, RIP provided the horizontal dot point coordinates of the four locations. RIP stores MM5 three and two-dimensional variables in binary files sorted by forecast hour. As it is with MM5 output, horizontal wind components are stored in arrays representing dot points and all other meteorological variables are stored in cross point arrays.

With this knowledge, a MM5 post processing program written in Fortran was used to pull vertical profiles of MM5 output for each of the four station locations and store the results in text format for input into Microsoft Excel. The variables pulled from the binary were: pressure, geopotential, temperature, horizontal wind components, and the mixing ratios for water vapor, cloud water, cloud ice, rain, snow, and graupel (in the case of Option 7). To account for MM5 reporting these variables at half sigma levels vertically and at cross points horizontally, the post processing program interpolated these

to full sigma levels and utilized an inverse weighted average scheme to interpolate from cross point or, if necessary, dot point coordinates to station location.

In order to compare MM5 output to archived upper air observations, a logarithmic interpolation feature of MATHCAD was employed. This method involved using existing mandatory and significant levels of RAOBs to predict temperature and humidity values at pressure levels corresponding to the MM5's sigma levels. With these data, residual plots of temperature and water vapor mixing ratio were computed for both cloud microphysics options at +12 hours and +24 hours of each forecast run. Residual plots representing zero hour analysis of the MM5 were also constructed, although it should be noted there is no difference in the initialization of MM5 utilizing either Reisner option since initialization is determined before the model employs these schemes.

Mention should be made of how the MM5 determines the height of the lowest terrain-following sigma level. In the model, the lowest sigma level is placed 20 meters above ground level. As Table 3 shows, there were differences between what the MM5 horizontally interpolated data points represented as ground level and the actual ground level of the verification sites. So, the lowest level of the residual plots calculated in this experiment correspond to the lowest sigma level of the model with temperature and

Table 3. Comparison of model and actual station elevations. Heights are given in meters above mean sea level.

Verification Site	Lowest MM5 Sigma Level	MM5 Station Elevation	Actual Station Elevation
Osan	74.91	54.91	12
Kwang-Ju	125.15	105.15	13
Wajima	123.94	103.94	7
Misawa	33.91	13.91	36

humidity values of the RAOB logarithmically interpolated to these levels. Diagnosis of winter precipitation based on model output uses this lowest sigma level as ground level.

MM5 forecasts of surface precipitation type were calculated in Excel with the output provided by RIP. Figure 7 presents a graphical representation of the method used in this study to determine precipitation type at the surface. Number concentrations, slope parameters, and fall speeds for all pertinent hydrometers were calculated in accordance with sections 2.4.2 and 2.4.3. To determine precipitation type at the surface, the

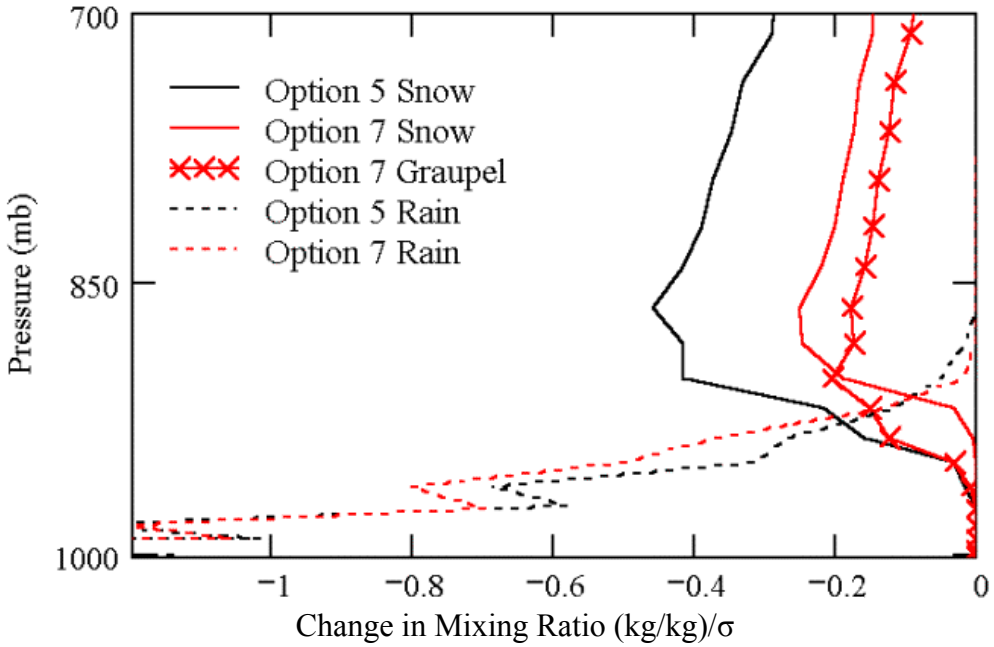

Figure 7. Example of the method used to determine precipitation type at the surface. Both options have a snowfall maximum between 900 and 850 mb and Option 7 graupel production is greater than that for snow beneath this layer. From approximately 950 to 850 mb, there is a mixed layer in which the frozen hydrometers completely melt into rain before reaching the surface.

hydrometric change in mixing ratio was calculated at sigma level 41. A fall rate greater than 2×10^{-10} kg/kg σ^{-1} indicated existence of snowfall at the ground level. If the graupel

fall rate was greater than 1 x 10^{-9} kg/kg σ^{-1}, in addition to being greater than the snow rate, ice pellets were predicted. Rainfall at ground level was predicted if the fall rate for the rain mixing ratio was greater than 0.01 kg/kg σ^{-1} (if the soil temperature was less than 0˚ C, freezing rain was the result). In this method, mixed rain and snow are allowed at ground level. Forecasts of precipitation type were verified against station surface observations at + 6, 12, 18 and 24 hours.

3.4. Test Design Principles

It is important to briefly discuss concerns involved in performing an experiment to statistically compare two MM5 cloud-microphysical schemes. The issues involved in test design include the pairing of sample forecast data and the temporal and spatial correlation of sample forecast errors. The methods used to categorically verify the forecast results of these two schemes are also detailed.

3.4.1. Pairing of Sample Data. Since winter precipitation forecasts of both Reisner schemes are based on the same model initialization, the hypothesis testing of this study treated Option 5 and Option 7 forecasts as paired sample data. The simultaneous forecasts of the two schemes were not considered independent groups but were treated as matched pairs that were correlated. Therefore, the use of the paired t-test was appropriate to compare differences of the group means (Hamill, 1998). Normal quantile plots of temperature and q_v residuals were interpreted to support the assumption of normality, a prerequisite necessary for using the t-test.

3.4.2. Temporal Correlation of Sample Forecast Errors. Research by Hamill, (1998) computed precipitation bias scores over a continuous 31-day period. This study

showed there was no evidence to indicate that precipitation forecasts 24 hours apart exhibit temporal correlation. This allows for the assumption of independence between forecasts 24 hours apart (00Z vs. 00Z or 12Z vs. 12Z). The Hamill study made no conclusion about forecasts separated by 12 hours. However, since it is possible that diurnal effects could corrupt meaningful verification results, particularly within the planetary boundary layer of the model, biases of 00Z and 12Z forecasts were computed separately.

3.4.3. Spatial Correlation of Sample Forecast Errors. An important issue that arises when verifying NWP forecast results for specific locations within a forecast domain is the degree of correlation between grid points (Hamill, 1998). For example, if the MM5 missed a snow event for Dayton, OH, it is also assumed to misrepresent the event for Columbus, OH because of the close proximity and similar topography of the two cities. Therefore, a sample of snow forecast verification results from both cities would show correlation and dependence. However, for this particular study, spatial correlation was not considered when evaluating results because the verification sites were not being compared to each other. Also, the appropriate techniques of multivariate analysis necessary to determine the degree of correlation between grid points would be intensive and would not particularly contribute to the goal of a physical assessment of model performance at each site.

3.4.4. Categorical Verification of Forecast Results. For each precipitation type, forecasts were partitioned into contingency tables of four mutually exclusive and collectively exhaustive events categorized by verification site, forecast option, forecast initialization, and forecast hour. Since the sample sizes of the experiment were relatively

small, the Fisher-Irwin Exact Test (FI) was used in place of the Chi-Square Test to determine if the MM5 forecasts were related in a meaningful way to the observed occurrences of precipitation. The measures used in this experiment for categorical verification can be illustrated using Table 4.

Table 4. Contingency table of possible events.

		Forecasts		
		Yes	No	
Observations	Yes	A	B	C
	No	D	E	F
		G	H	I

The skill of a model or any other forecast process is a measure of its ability to accurately predict above what would be expected by chance or climatology (Panofsky and Brier, 1968). To test the skill of the MM5 to categorically forecast precipitation types at the surface, the Heidke Skill Score (HSS) was used. HSS accounts for categorical verification due to chance (Stanski et al., 1989). A "hit" due to chance is given as the event frequency multiplied by the number of forecasts. The equation for HSS given by Panofsky and Brier (1968) is:

$$HSS = (A + E - Z)/(I - Z) \qquad (15)$$

where Z is the hits due to chance, which is calculated using the marginal probabilities:

$$Z = (CG + FH)/ I \qquad (16)$$

Thus, a HSS greater than zero indicates the model is performing better than chance alone and shows forecast skill. A HSS of zero or less indicates the model performed the same or worse than what was expected by chance alone, thus, showing no skill.

In addition to forecast skill, bias scores were used to measure the correspondence between the MM5's forecasts and the observed occurrences of precipitation. This method is defined by (Colle et al., 1998):

$$\text{Bias} = (A + B) / (A + D) \qquad (17)$$

A bias greater than 1 indicates over prediction, while a bias less than 1 indicates under prediction.

IV. Results and Analysis

4.1. Initialization of Temperature and Moisture Fields

The observational analyses used by the MM5 in this experiment were horizontally interpolated to each of the four verification sites. Figure 8 shows the results of model initialization at Kwang-Ju during the study period that was typical at all verification sites. Overall, the analysis of initial temperatures showed a significant +0.5ºC average warm bias throughout most of the troposphere. In the upper troposphere, above the 300 mb level, this warm initialization bias increased to between 1 and 2ºC. The only site where the MM5 tended to initialize too cold in the middle troposphere was at Wajima, which experienced a significant average –0.25ºC bias from 800 to 400 mb at both 00Z and 12Z. Statistical analysis of the average of the surface temperature initializations at most of the verification sites failed to detect a significant temperature bias at the lowest sigma level since the residuals were too widely scattered about the means. However, the model usually initialized surface temperatures within ±1 ºC of the RAOB.

As the example in Figure 8 shows, t-test results performed on the initialization of the moisture fields showed less firm evidence of bias in the analysis of water vapor. This lack of evidence is probably related to inherent difficulties of RAOBs to accurately measure humidity (COMET, 1998). The humidity profile of the atmosphere can show very abrupt changes in the vertical and horizontal compared to the temperature field. Humidity sensors are prone to high measurement errors particularly within the upper troposphere and these errors vary according to the model of the radiosonde used. In model verification, these humidity errors can be compounded by the vertical resolution of

the model. Although the number of sigma levels used in this experiment was relatively large compared to previous research by other authors, the model might have lacked the layers to adequately determine fine differences in the humidity field.

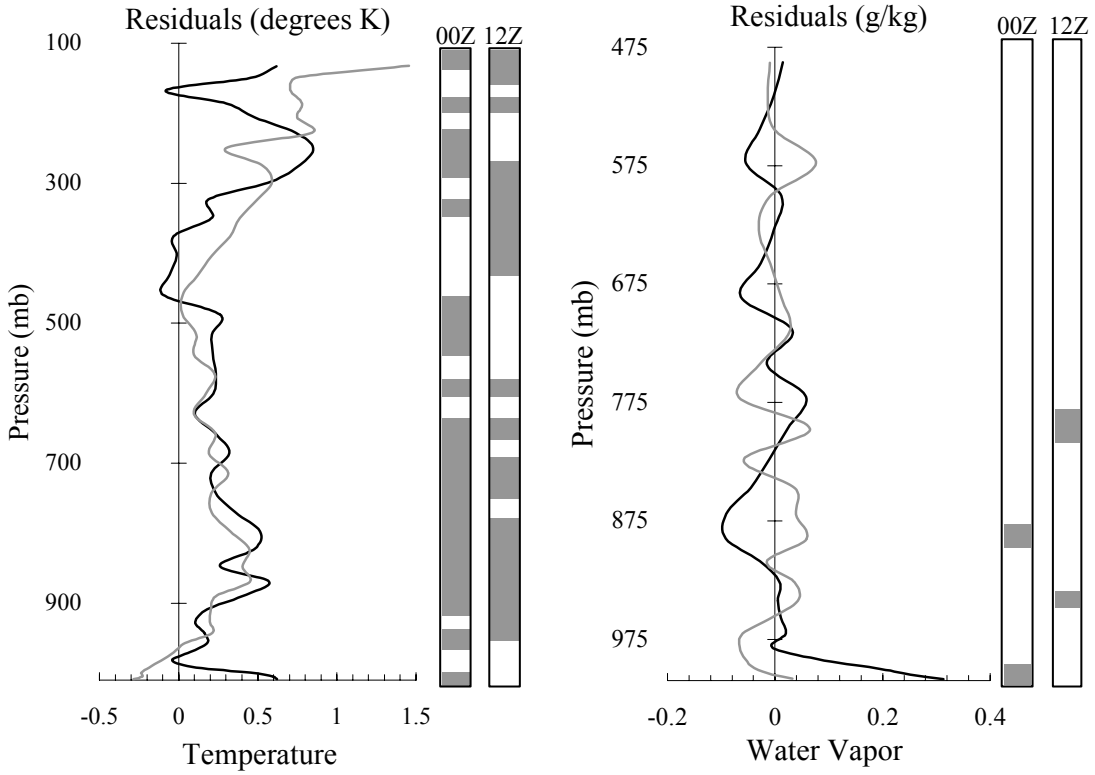

Figure 8. MM5 initialization at Kwang-Ju AB during the experiment (00Z analyses are represented in black and 12Z analyses are in gray). The filled bars indicate those levels where the average interpolated 00Z and 12Z MM5 analyses were significantly different from each station RAOB at 90% confidence according to Student's t-test for paired data.

4.2. Observations of Cloud Ice and Cloud Water Production.

The study demonstrated that Option 5 generates far more cloud ice in the upper levels of the atmosphere compared to Option 7. As stated previously, Option 5 prescribes ice production by using a form of the Fletcher curve that doesn't place a lower

temperature bound, while Option 7 places a lower limit of -27 ºC. The Option 5 model runs generated maximum ice by the 6-hour forecast point, and this ice remained in the upper troposphere from 400 to 300 mb throughout the model run. This over production of ice cloud was consistent with previous studies over the U.S (Manning and Davis, 1997). As the example in Figure 9 shows, this cloud ice generally covered much of the model domain. In contrast, the Option 7 averages in maximum q_i were far less and the scheme did not generate extensive ice cloud.

It first appeared that the ice concentrations of both schemes contributed to the warm bias that increased in the upper troposphere toward the 24-hour point of both the 00Z and 12Z runs. However, there does not appear to be evidence that the warm bias was the result of the cloud ice trapping shortwave radiation in the upper troposphere, since the Option 7 temperature errors aren't significantly less than the Option 5 errors at these heights. As hypothesized by Manning and Davis (1997), the warm bias might be related to the resolution of the sigma levels. Although the East Asian window used in this experiment had 41 sigma levels, there were only about 8 of these to cover the vertical distance from 400 to 200 mb. It's possible the model was often unable to resolve the drastic change in temperature lapse rate that typifies the tropopause.

Although too cold to directly produce snow or graupel, the cloud ice maximum in the upper levels of wintertime nimbostratus is a significant source region for ice crystals that are converted to frozen precipitation in the lower levels. Conversion to snow and graupel by collection or riming of ice typically occur at altitudes where temperatures are between –4º and -10º C and where large concentrations of ice particles coexist with supercooled cloud water. The study showed these levels averaged secondary maxima in

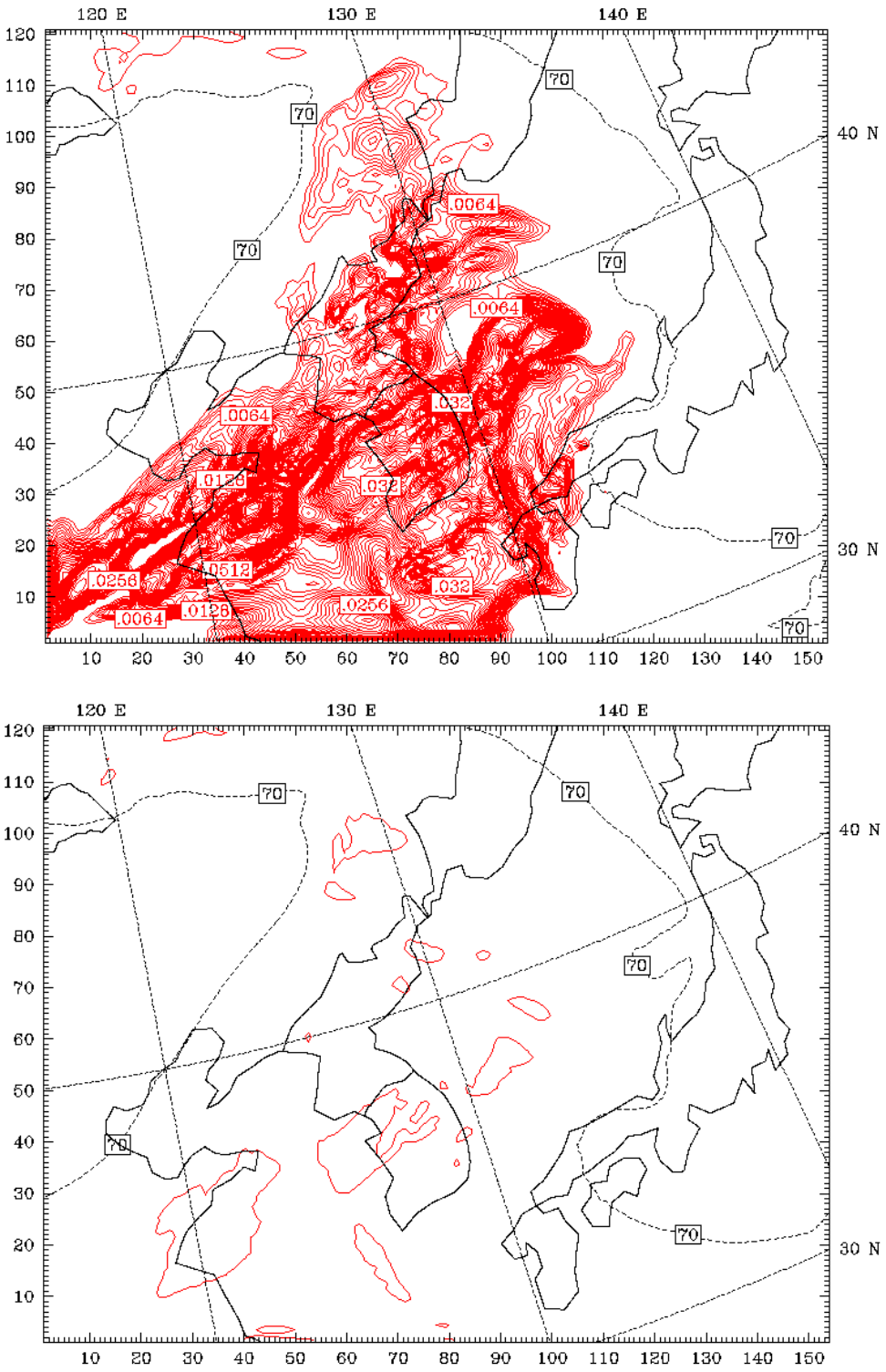

Figure 9. Illustration of the difference in Option 5 (top) and 7 (bottom) cloud ice production. The above charts are 12-hour forecasts valid 17 Jan 98 at 00Z and depict q_i at the 400 mb level. The contour interval is every 0.0016 g/kg. The dashed line enclosing the areas of q_i represents the 70% relative humidity level with respect to ice.

ice particle concentration; however, the Option 5 number concentration was still several orders of magnitude greater than Option 7 at Misawa, Osan, and Kwang-Ju. Because Option 7 places an upper bound on ice concentrations proportional to q_v, the scheme prevented significant ice generation, except at Wajima, which had higher average q_v values in the lower troposphere. Appendix B provides model averages in cloud ice for each verification site during the period of study.

It was hypothesized by Manning and Davis (1997) that overproduction of cloud ice contributed to average cold biases within the PBL over the western U.S. by preventing shortwave radiation from reaching the surface. However, the disparate Option 5 and 7 ice production simultaneous with similar vertical temperature biases suggest surface soil processes and land-sea interactions play a far more prominent role in the cause of daytime low level temperature biases within the East Asian domain.

Option 7 tended to generate higher amounts of water vapor and more cloud water (a consequence of having more vapor available for condensation). Option 5 as currently employed by AFWA is known to over predict clouds at the 850 mb level particularly over ocean areas (MetEd, 2002). Therefore, although no direct verification of q_c was performed, it is suggested that Option 7 has operationally less desirable results in terms of liquid cloud production during the period of study.

4.3. Verification Results for Osan AB.

4.3.1. Comparison of Forecast Skill at Osan AB. Measurable amounts of snowfall fell at Osan on seven days during the period of study. There were 5 consecutive days of snow during the first half of the study period. The most significant snowfall occurred on

08 Jan 98 when a total of 13.2 inches of snow fell at the base. No occurrences of rain or ice pellets were observed at Osan during the 20-day record of surface observations.

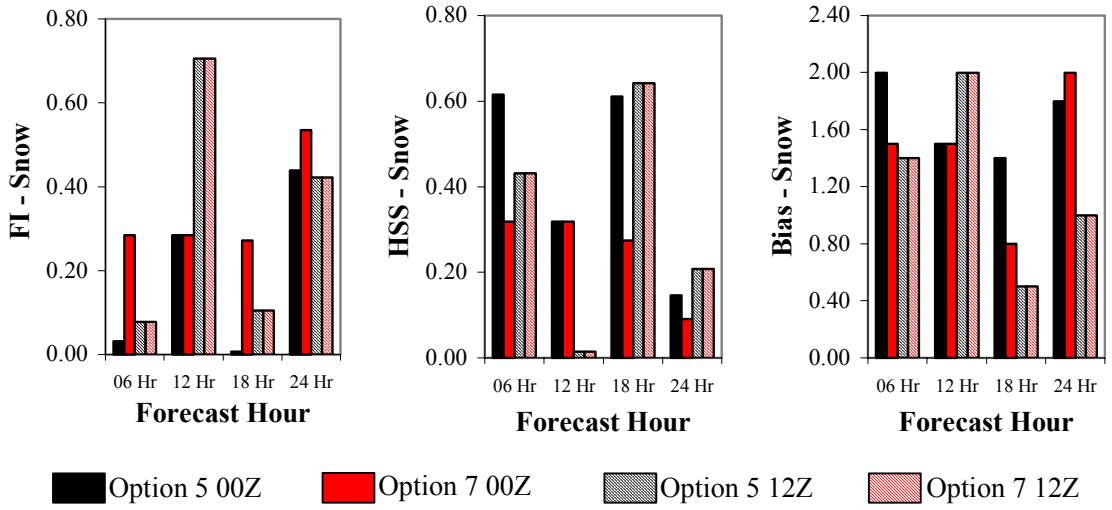

Figure 10. Categorical verification measures for Osan AB.

As shown in Figure 10, Option 5 provided significantly more meaningful forecasts of snow at Osan for forecasts initialized at 00Z. Results for the 12Z model runs were equal and generally less accurate. Overall, the MM5 had the best performance at +06 and +18 hours. Both Reisner schemes displayed the worst performance during forecast hours that were valid at 09L (+24 hours for 00Z initializations and +12 hours for 12Z initializations). These hours of poor skill coincided with a +200% bias in the prediction of snow.

4.3.2. Hypotheses Regarding Forecast Errors at Osan AB. The MM5 forecasts for Osan tended to be marked by a deep cold bias in the lower troposphere and a warm bias above 900 mb. The low-level temperature bias was of lesser extent during the morning hours, yet still exhibited the diurnal characteristics shown by Manning and Davis (1997) who hypothesized that these boundary layer errors are related to the MM5's

PBL scheme. Both options generated maximum cloud water (Option 7 producing the greater amount) during the afternoon and early evening hours.

When model results for Osan were interpolated to the morning soundings of the case period, both cloud microphysics schemes performed the same: displaying a cold and dry bias in the lower levels and a warm/moist bias in the middle troposphere. The moist bias appeared during the minimum of cloud water highlighting the inverse relationship of q_v and q_c through the processes of evaporation and condensation. The MM5's mid-tropospheric warm bias, apparent during the morning and evening, is probably the result of the model's cloud and free atmosphere radiation processes or wind biases that affect temperature through the process of advection (Manning and Davis, 1997).

When model results were interpolated to the nighttime soundings of the case period, the MM5 forecasted atmosphere was too dry throughout almost the entire column. The 12Z RAOBs coincided with the maximum cloud water of the afternoon and early evening hours. Opposite of what was observed during the day, the nighttime results showed a significant difference in low-level q_v bias between the two cloud microphysics schemes and this difference appeared to be linked to the production of cloud water and frozen precipitation. As shown in Figure 11, the nighttime forecast hours (particularly 12Z + 24 hours) showed an abrupt decrease in q_s and q_g beneath the maximum in cloud water indicating rapid evaporation. The less humid a layer of atmosphere is beneath a saturated layer of cloud and precipitation, the greater the effect of evaporative cooling. The significant difference between the two schemes (Option 7 being more moist) appears to be the consequence of Option 7 averaging more cloud water except at the level of

12Z + 12 hours (valid 0900 local time)

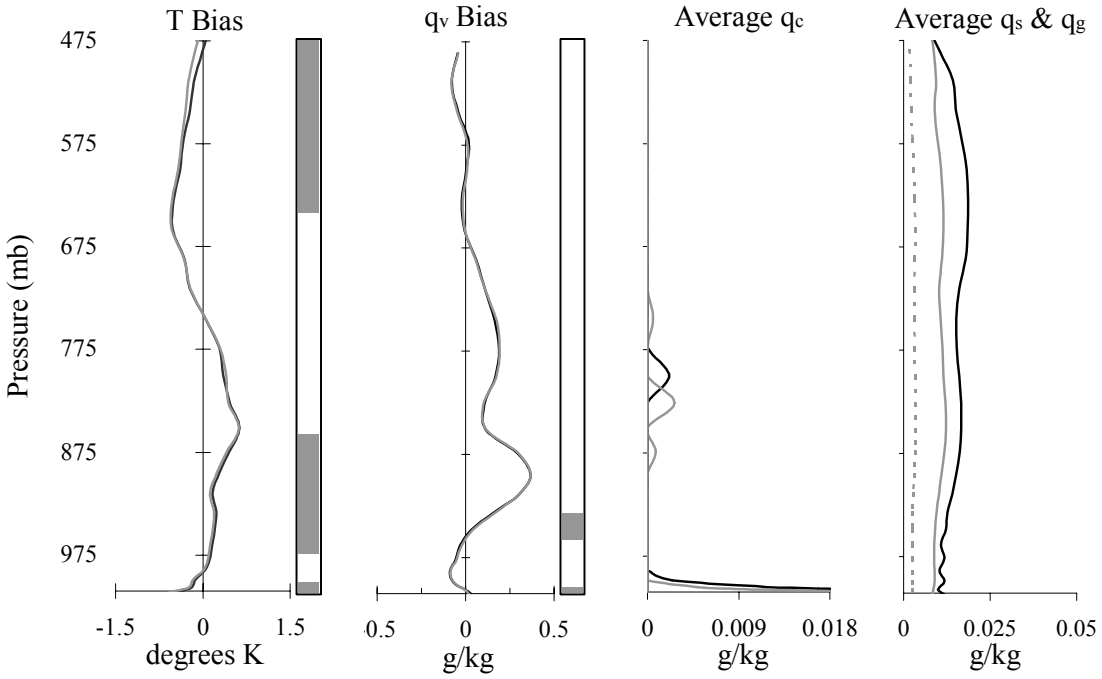

12Z + 24 hours (valid 2100 local time)

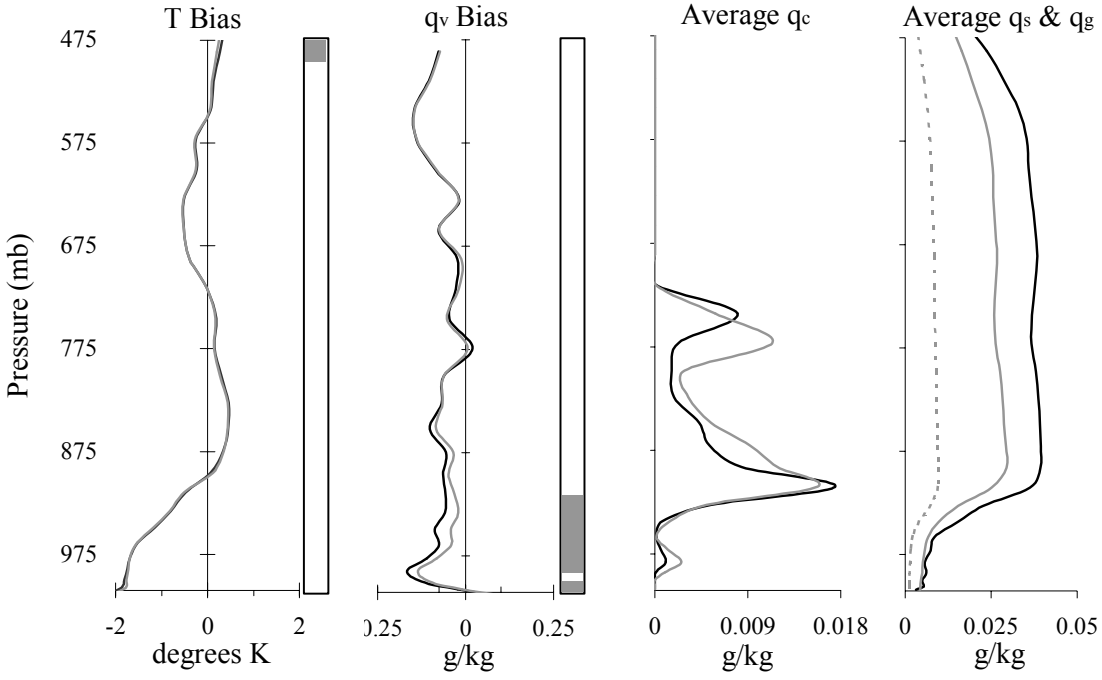

Figure 11. Average 12Z interpolation results for Osan AB. The filled bars next to the temperature (T) and q_v plots indicate the levels where Option 5 (black) and Option 7 (gray) are significantly different at 90% or greater confidence (q_g is depicted as a dashed line).

maximum frozen precipitation production. The rapid drop off of Option 7 q_c suggests that riming processes are contributing to a higher rate of cloud water depletion, increasing the rate of evaporative cooling in the subsaturated layer, thus increasing the moist bias.

The production of snow at Osan during the experiment appeared to be directly influenced by cloud water availability. The overproduction of snow during morning hours due to rapid depletion of cloud water contributed to the low forecast skill of both cloud microphysics schemes during forecast hours valid at 00Z (09L) with Option 5 having only slightly better performance. However, a minimum in snow and graupel production was observed at forecast hours coinciding with 06Z (15L). This minimum coincides with the daytime spin up of the q_c field where it appears the snow and graupel fields have not had enough time to generate through depletion of cloud water. Therefore, there was less snow over prediction bias, resulting in a more realistic simulation of the actual snow fields at Osan AB during the afternoon hours.

4.4. Verification Results for Kwang-Ju AB

4.4.1. Comparison of Forecast Skill at Kwang-Ju AB. Snow fell at Kwang-Ju on six days during the period of study, the majority of which fell late in the period. There were also significant occurrences of rainfall, which happened on five days. No occurrences of ice pellets or freezing rain were observed.

As the results in Figure 12 show, there was not an appreciable difference in the ability of two cloud microphysics schemes to determine precipitation type at Kwang-Ju during the period of study. Both microphysics options overall produced too much snow

at Kwang-Ju and generally there was no difference in snow bias between the schemes except at +18 and +24 hours of the 12Z forecast runs where Option 7 showed no bias.

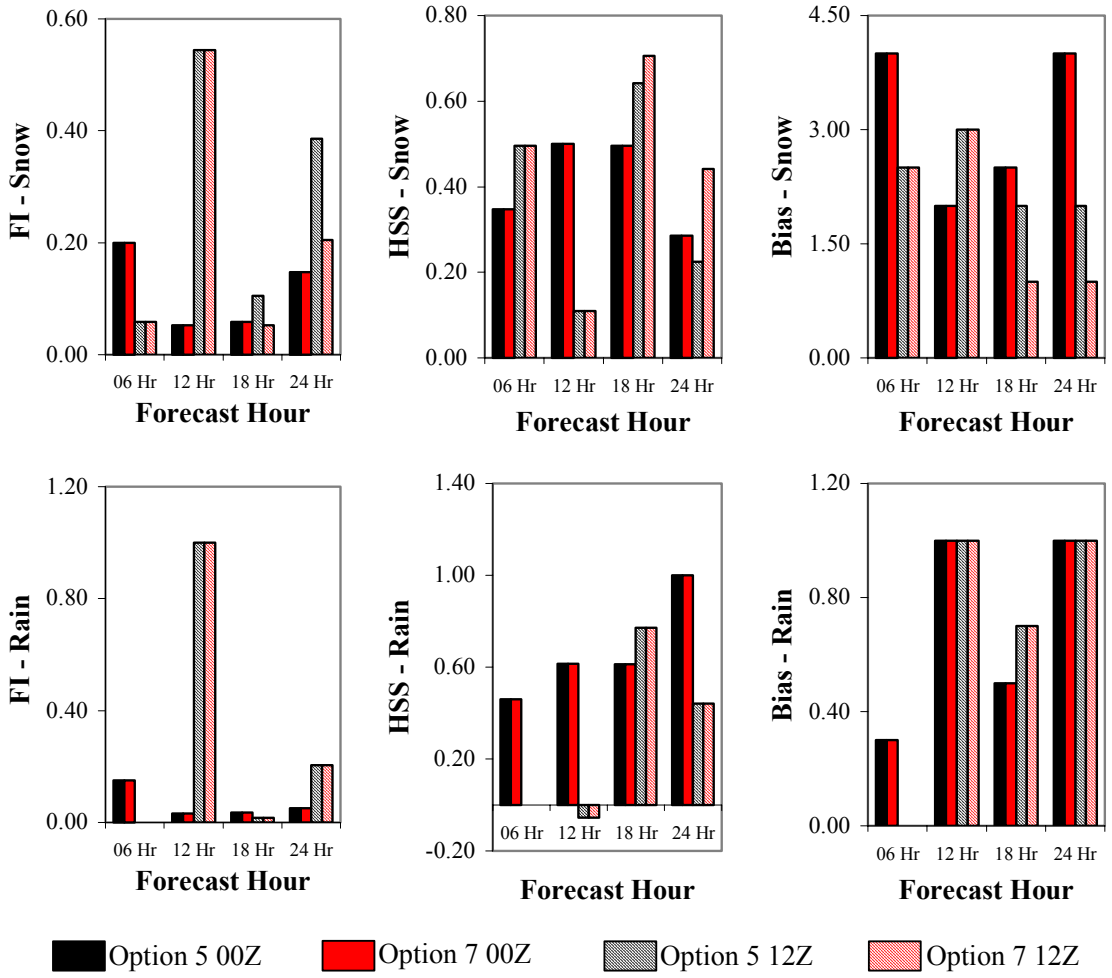

Figure 12. Categorical verification measures for Kwang-Ju AB.

The MM5 had better performance handling rainfall with both schemes acting equally. The low skill at 12Z+12 hours is the result of over prediction of snow and mixed precipitation combined. Both options created too much mixed precipitation at the surface at Kwang-Ju at all forecast hours. During the study period, the model predicted mixed precipitation on a total of 11 occasions of which none verified (the actual result was rain

in most cases). One 12Z +12 hour Option 7 forecast resulted in ice pellets, which also did not verify.

4.4.2. Hypotheses Regarding Forecast Errors at Kwang-Ju AB. Opposite of what was observed at Osan, Figure 13 shows that MM5 forecasts for Kwang-Ju typically had a warm bias in the lower levels above the PBL and a cold bias in the middle levels of the troposphere. This pattern was characteristic of all forecast hours although the errors had a greater magnitude during the evening. When compared to evening soundings, which are representative of conditions 2½ to 3 hours after sunset at Kwang-Ju (presumably before the full impact of radiational cooling at the surface), the MM5 PBL tended to be too cold. The morning soundings representative of conditions 1 to 1½ hours after sunrise (before the full effect of daytime heating) showed a better resolution of PBL temperatures with Option 7 giving slightly better results.

Generally, the MM5 forecasts for Kwang-Ju were too moist below 800 mb during all hours. There also appeared to be a diurnal pattern to the observed humidity errors within the PBL. Interpolation of both Option 5 and 7 forecasts to the Kwang-Ju 00Z RAOBs showed that the average humidity bias decreased sharply toward the top of the PBL in conjunction with the decreasing cold bias. Also different from what was observed for Osan, the MM5 at Kwang-Ju consistently forecast cloud water during all hours within Option 7 producing the greater amount.

At Kwang-Ju, Option 5 produced more snow in the upper levels where there was little q_c and most snow generation was the result of conversion and collection of cloud ice. However, in the lower levels where mixed phase processes are more important, Option 7 produced more combined frozen mixing ratio ($q_s + q_g$) than Option 5 q_s. This is

00Z + 12 hours (valid 2100 local time)

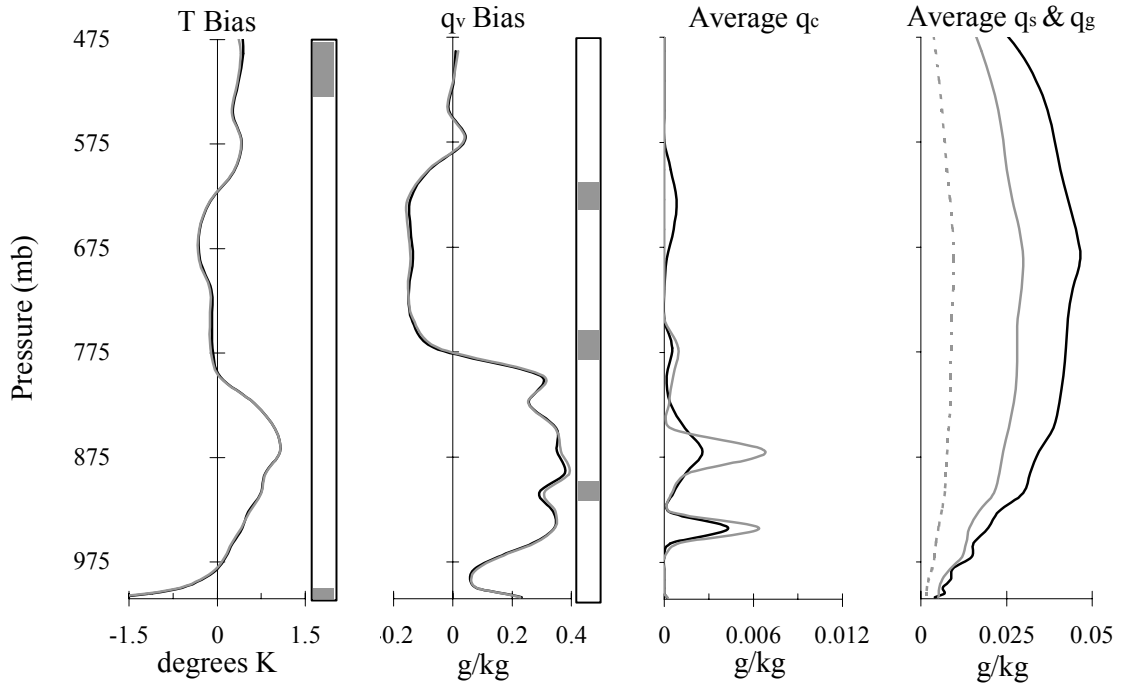

00Z + 24 hours (valid 0900 local time)

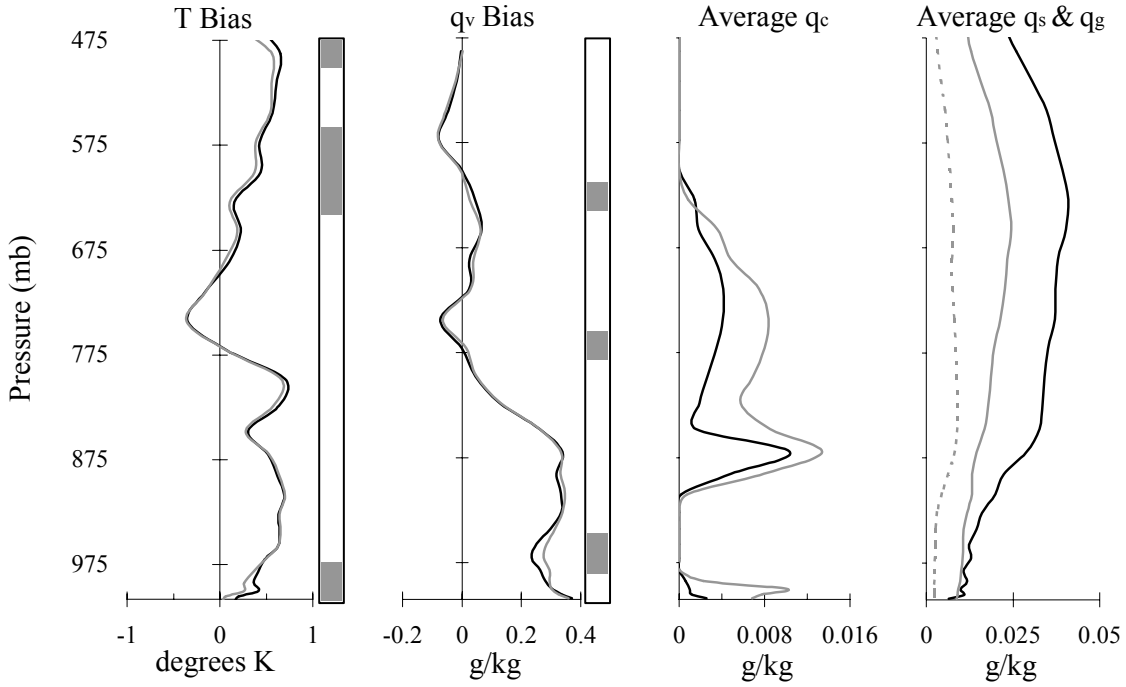

Figure 13. Average 00Z interpolation results for Kwang-Ju AB. The filled bars next to the temperature (T) and q_v plots indicate the levels where Option 5 (black) and Option 7 (gray) are significantly different at 90% or greater confidence (q_g is depicted as a dashed line).

a consequence of Option 7 producing more cloud water. The Option 7 snowfall produced more evaporation in the subsaturated layer beneath the average cloud cover causing average q_v for the scheme to be higher, particularly during the morning hours. The cold bias at the surface during the evening hours combined with an approximate 100 meter difference in height between the lowest sigma level and Kwang-Ju's station elevation likely did much to keep some snowfall from completely melting, contributing to both schemes disappointing skill in forecasting mixed precipitation at the site. Overall, despite the differences in snow production, the fact that both schemes over produced snow meant that neither had an advantage over the other in accurately predicting precipitation type at Kwang-Ju during the time period of the study.

4.5. Verification Results for Wajima

4.5.1. Comparison of Forecast Skill at Wajima. Due to its location, which situates the city in the path of rapidly moving extra-tropical cyclones and instabilities resulting from onshore effects from the Sea of Japan (details given in Appendix A), Wajima received precipitation during most days of the study. This precipitation fell in wide variety of forms: rain, snow, mixed, and ice pellets were all observed. Overall, the MM5 showed poor ability in handling the rapidly changing conditions and precipitation types observed at Wajima and this weak performance was the result of both cloud microphysics schemes over predicting mixed precipitation. As shown in Figure 14, some of the average forecasts of both options actually showed a negative skill in predicting precipitation type, meaning the scheme performed worse than if the forecasts were

determined entirely by chance alone. At Wajima, similar numbers of mixed precipitation forecasts produced during the experiment resulted in either rain or snow, thus exposing the inability of both schemes to realistically simulate both the melting and evaporation of frozen precipitation at the site.

4.5.2. Hypotheses Regarding Forecast Errors at Wajima. As shown in Figure 15, the averages of the MM5 forecasts for Wajima during the period displayed similar features regardless of forecast hour. There was typically a 1ºC warm bias in the surface layer, a slight cold bias in the immediate layer above the PBL, and a slight warm bias throughout the middle troposphere. The consistent surface warm bias could be related to the modifying effects of the model's analyses of the surrounding sea surface temperatures. The low level warm bias by itself would produce higher rates of melting of frozen precipitation and is the likely contributor to the large number of mixed precipitation forecasts in which the actual result was rain.

Wajima was unique among the verification sites used in the study for the massive amounts of all the cloud microphysics variables produced by the MM5. The average forecast soundings for the site displayed larger and more equitable amounts of cloud ice in the middle levels of the troposphere where mixed phase processes are important. Also, the average amounts of cloud water were several times larger than what was observed at the other verification sites. This abundance of cloud ice and supercooled liquid water within the mixed phase layer of the model led to increased production of snow and graupel through the riming of cloud ice.

Option 7 produced the largest amounts of q_g at Wajima during the study providing evidence that the scheme is sensitive to locations within its domain where graupel

processes are important. The average combined frozen mixing ratio of Option 7 was often greater than Option 5 q_s, particularly close to the surface where Option 7

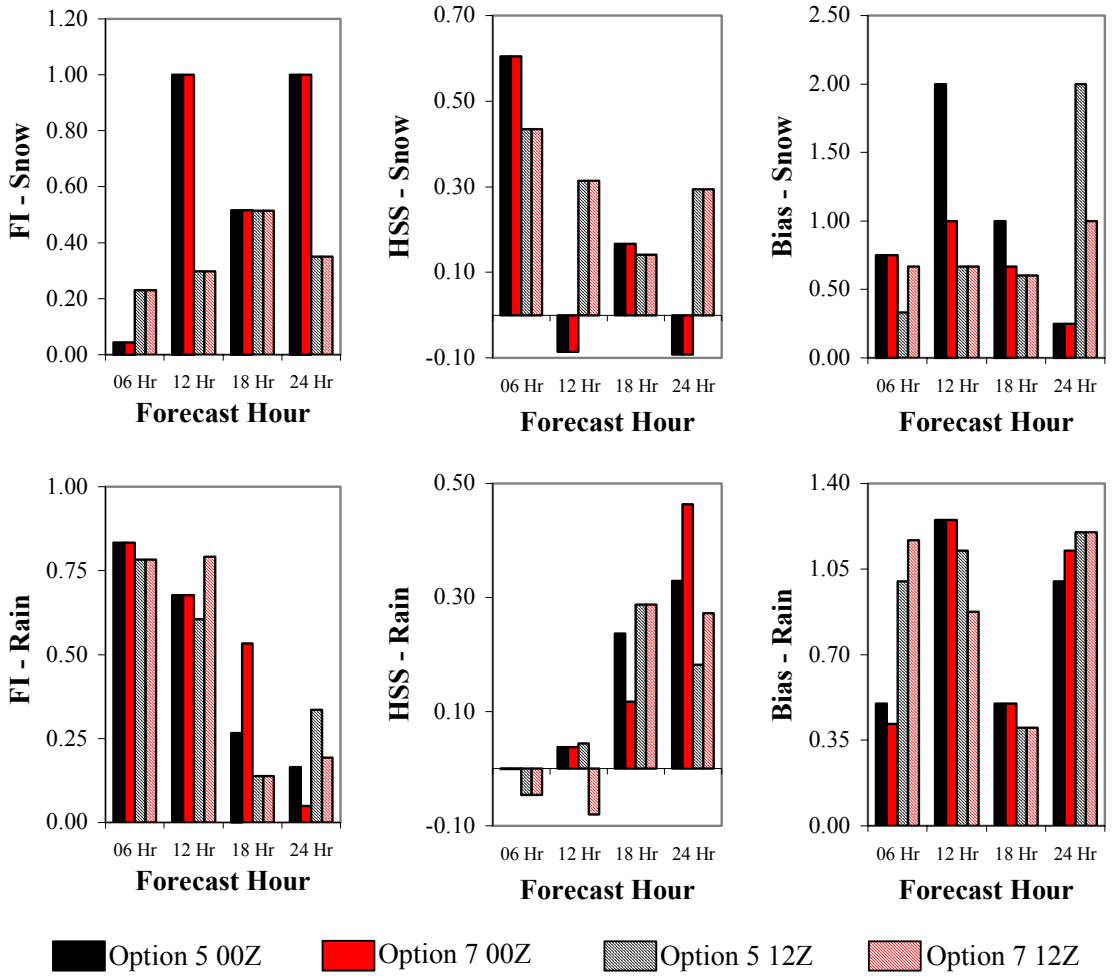

Figure 14. Categorical verification measures for Wajima.

tended to produce more graupel than snow. The warmer surface temperatures meant that most graupel was converted to snow instead of ice pellets, because the scheme only allows snow to exist in temperatures above freezing. However, the two actual occurrences of ice pellets at Wajima during the 20-day period happened when surface temperatures were above freezing. The MM5 forecast soundings for Wajima also

00Z + 12 hours (valid 2100 local time)

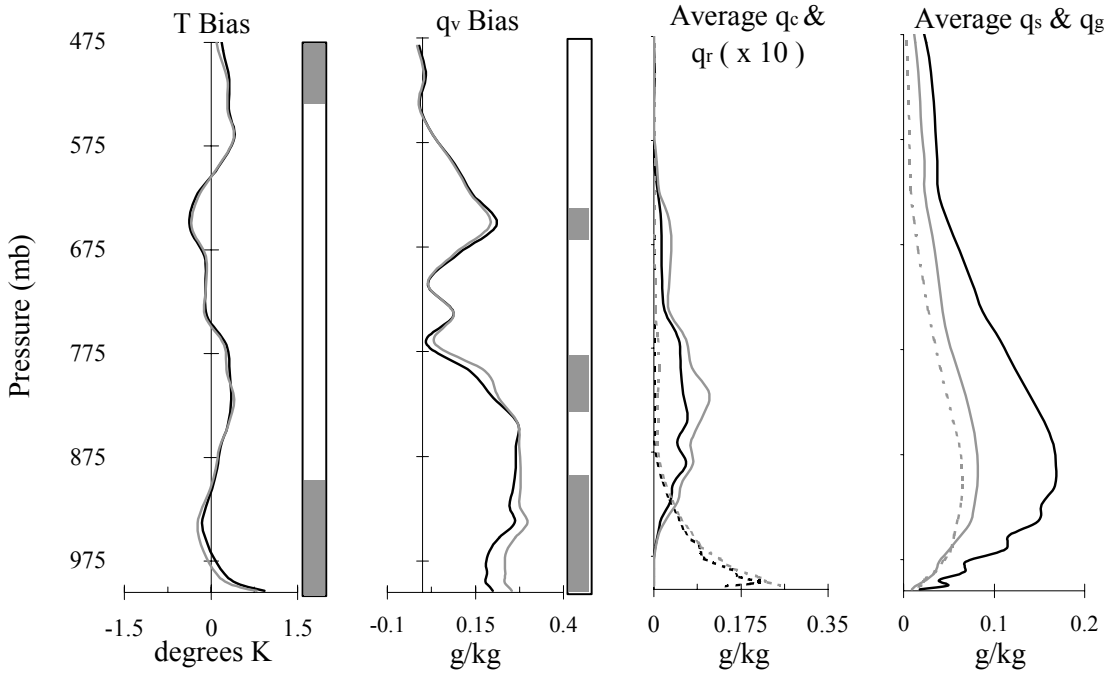

00Z + 24 hours (valid 0900 local time)

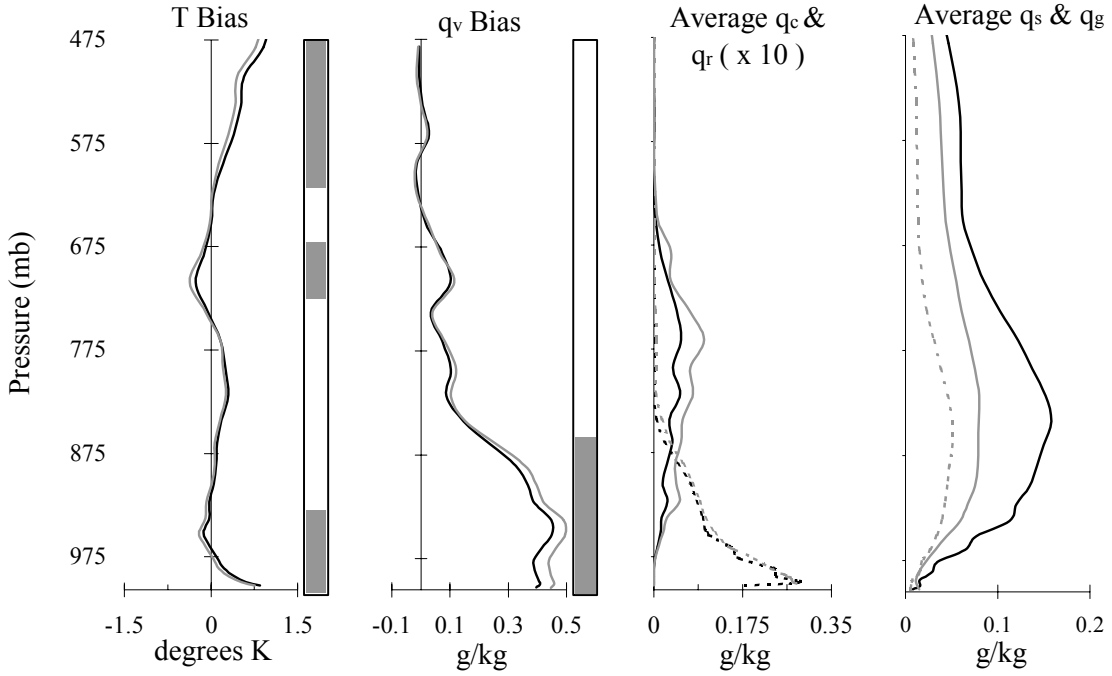

Figure 15. Average 00Z interpolation results for Wajima. The filled bars next to the temperature (T) and q_v plots indicate the levels where Option 5 (black) and Option 7 (gray) are significantly different at 90% or greater confidence (q_r and q_g are depicted as dashed lines).

produced greater amounts of rain compared to the other verification sites. The Option 7 rain was always greater in the lower levels, particularly at the surface.

The greater amounts of rain and frozen precipitation produced by Option 7 account for that scheme's significantly greater moist bias in the low levels at Wajima. However, for both options, the large moist bias created a decreased wet-bulb temperature profile than actually existed in the real atmosphere. The result was less evaporation of snow, which is likely a major contributing factor to the high number of mixed precipitation forecasts resulting in snow observed at the site.

4.6. Verification Results for Misawa AB

4.6.1. Comparison of Forecast Skill at Misawa AB. During the 20-day period of study, Misawa received 12 days of recorded snowfall totaling a combined amount of 123 inches. Overall, both Option 5 and 7 provided meaningful forecasts of precipitation type at hours in which the model displayed no bias or a slight under prediction bias in snow production. However, as shown in Figure 16, forecast hours valid at 06Z (15L) performed poorly. For both options, the successful number of hits at 18Z was smaller than what would be expected by chance alone even though the number of snow forecasts matched the number (but not timing) of observed occurrences of snow.

4.6.2. Hypotheses Regarding Forecast Errors at Misawa AB. The averages of the MM5 forecasts for Misawa during the period displayed similar profiles when interpolated to the station's 00Z and 12Z RAOBs. In the morning and evening, the MM5 generally had a warm bias in the boundary layer. However, the daytime MM5 boundary layer appeared too cold when forecasts of temperatures were compared to the 18Z Misawa

surface observation. At all hours the MM5 tended to be too moist in the lower levels with a significant difference in the bias of the two cloud microphysics schemes (Option 7 being more moist). In conjunction with the cold bias at 18Z, this moist bias created a

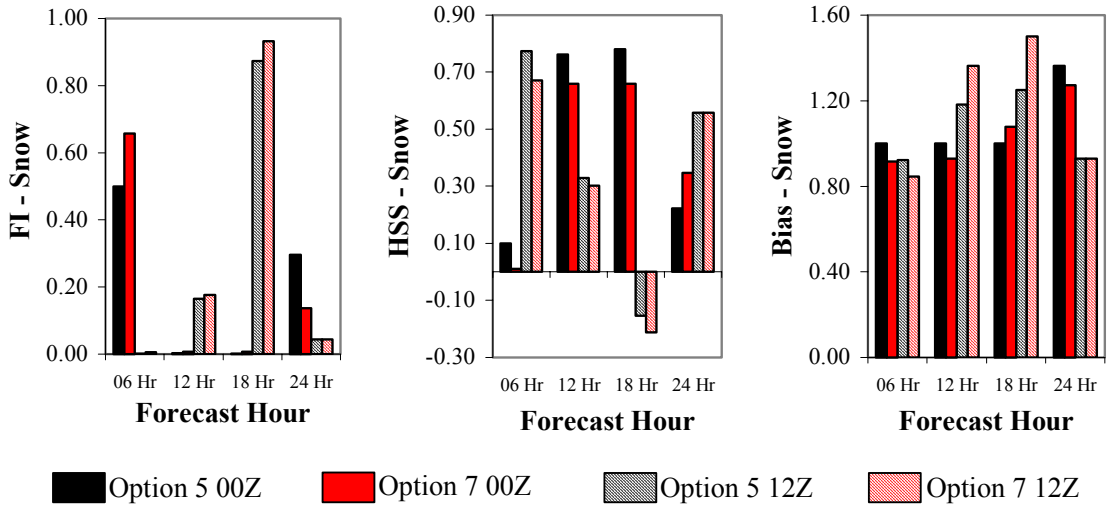

Figure 16. Categorical verification measures for Misawa AB.

decreased wet-bulb profile at the surface. On 11 forecasts corresponding to 18Z, both options forecasted snow while the actual result was no precipitation at all. This indicates the combined cold and moist bias tended to prevent snow from evaporating and played a large part in the MM5's low skill during the afternoon hours at Misawa.

Compared to the other verification sites, Misawa averaged a large secondary maximum in Option 5 ice production in the layer between 800 and 600 mb. Consequently, the average region of mixed phase precipitation processes was deeper at the site. As shown in Figure 17, there was a consistent layer of cloud water with Option 7 generating approximately 50% more q_c during all forecast hours. The largest

12Z + 12 hours (valid 0900 local time)

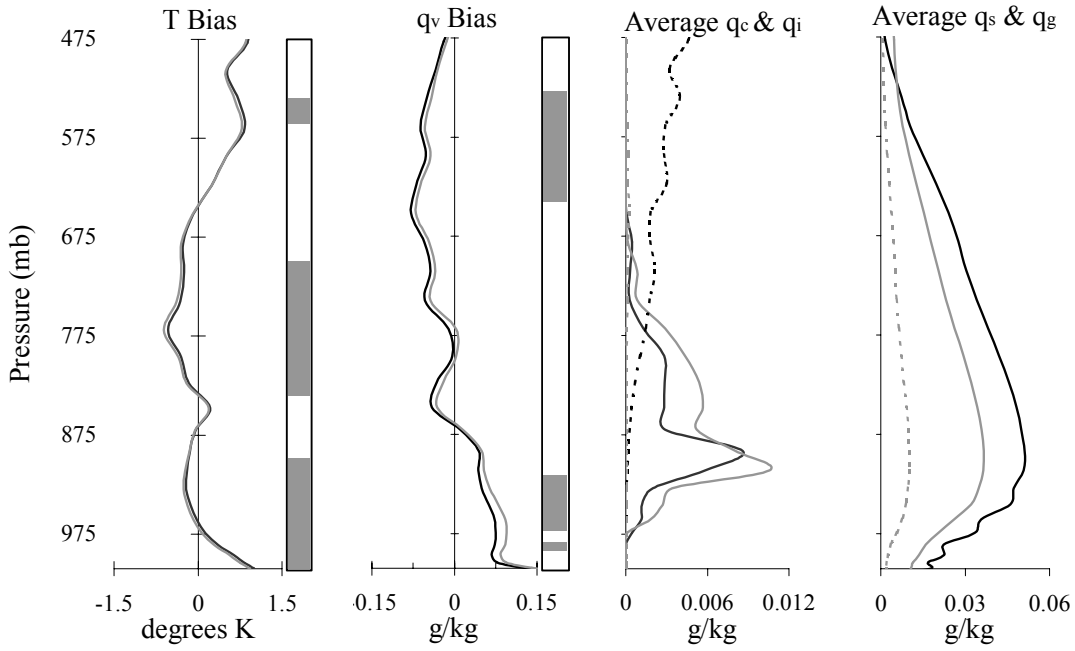

12Z + 24 hours (valid 2100 local time)

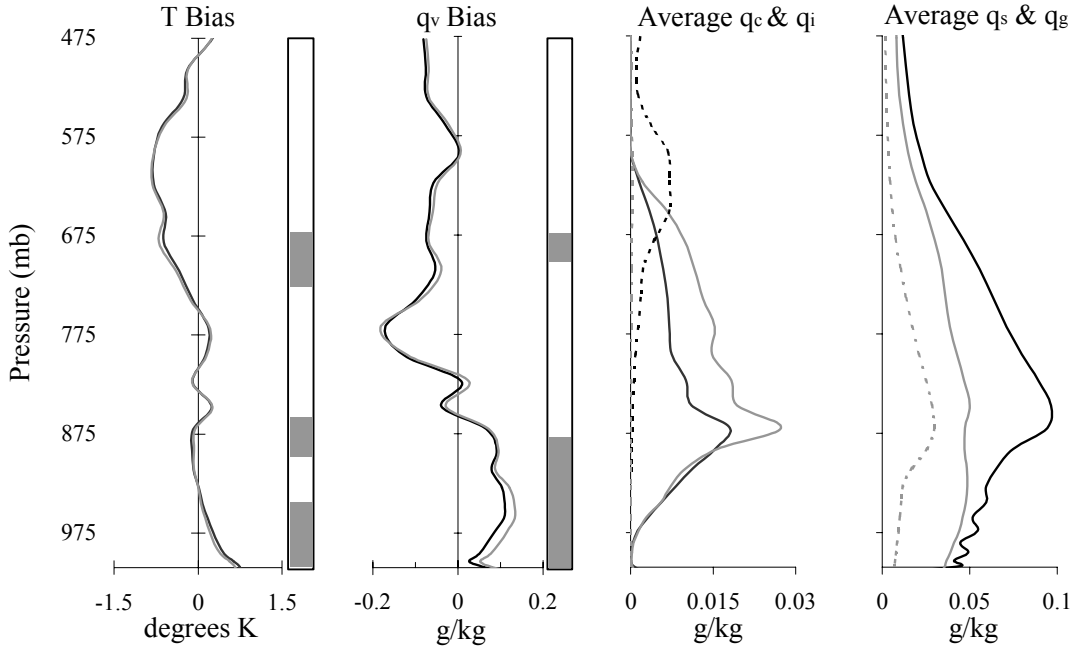

Figure 17. Average 12Z interpolation results for Misawa AB. The filled bars next to the temperature (T) and q_v plots indicate the levels where Option 5 (black) and Option 7 (gray) are significantly different at 90% or greater confidence (q_i and q_g are depicted as dashed lines).

differences in moist bias between the two schemes occurred beneath the maximum of cloud water and coincided with the layers of maximum snow and graupel evaporation.

The differences in cloud ice and cloud water between the two schemes meant that conversion and collection of ice played a more important role in Option 5 snow production, while accretion, collection, and riming associated with supercooled liquid water dominated the frozen precipitation production of Option 7. Option 5 tended to generate more snow aloft with the difference of the two being Option 7 graupel production. Option 7 predicted ice pellets on 11 occasions, yet no occurrences of this precipitation type were recorded. Since snow bias of the schemes weren't significantly different, the overproduction of graupel resulted in Option 7's weaker performance at the site during the period of study. These findings suggest Option 7 riming and graupel processes do not predict winter precipitation development at Misawa well.

V. Conclusions and Recommendations

5.1. Conclusions

The main purpose of this study was to gain an understanding of the limitations of the MM5 cloud microphysics parameterization currently used by AFWA and make a recommendation as to whether a more computationally expensive scheme would be better suited for the East Asian theater. The ultimate goal was to find a way to reduce the negative impact winter precipitation places on military operations and public safety. The motivation behind testing the Reisner Mixed-Phase Graupel Scheme was to determine if graupel and riming processes would have positive outcomes in producing more realistic forecasts of winter precipitation for Japan and Korea.

The research objectives listed in the introduction of this document as being necessary for the achievement of the main goal of this thesis were greatly met. The case period from January 1998 was marked by the passage of several extra-tropical cyclones that provided an ample observational database for a MM5 verification study. The East Asian MM5 domain window was successfully set up to run on the processors of AFIT's meteorology lab and the monumental task of generating two one-way nested MM5 runs for every 12 hours of the 20-day case period was accomplished. The weighted average and logarithmic interpolation methods employed to compare gridded MM5 fields to the radiosonde observations of the four verification sites proved more than adequate, thus enabling a thorough statistical comparison. The t-test was a useful tool for detecting regions in the vertical column of the atmosphere where the two cloud microphysics schemes were significantly different. Together, the Heidke Skill Score and the Bias

Score proved to be practical methods to categorically evaluate the MM5's ability to predict surface precipitation type.

The main results of this research show both cloud microphysics schemes are correlated in that they exhibit the same trends in temperature and humidity errors. This correlation is expected since both schemes have the same initial condition, are responding to the same grid-scale dynamical processes of the MM5 (such as advection), and are also responding to other below grid-scale parameterizations within the model (PBL, cloud radiation, etc.) However, the schemes showed significant difference in the magnitudes of humidity errors within the lower atmosphere of the model. The tendency of Option 7 to be more moist appears related to its significantly greater generation of cloud water. This unequal generation of cloud water in addition to differences in cloud ice production meant that conversion and collection of ice dominated Option 5 winter precipitation processes while accretion, collection and riming associated with supercooled liquid water dominated those of Option 7.

The overall conclusion of this research is that AFWA should not alter the cloud microphysics scheme (Option 5) currently employed to determine winter precipitation type for its East Asian forecast window. Of the four verification sites used in this study, Option 5 clearly had better performance at two of these locations, while at the others, neither scheme showed an advantage. This research provides evidence that the inclusion of Option 7 graupel and riming processes will not increase the skill of the MM5 to determine winter precipitation type within this model domain and would actually have negative operational impacts if employed within the model.

5.2. Recommendations for Future Research

The task of gathering a sample to cover a 20-day period required 160 MM5 runs with each run typically taking 6 hours to process using the computational capabilities of the AFIT meteorology lab. Limitations in time and resources meant that a more comprehensive study of the MM5's cloud-microphysics parameterization schemes could not be accomplished. However, because of the USAF's increasing reliance on NWP, the need for future verification studies outside the continental U.S. is very apparent. To further expand on the research presented in this thesis, the following recommendations are offered:

1. Statistical verification for this experiment was a challenging endeavor and relied on simple measures such as skill score and the t-test. Although these techniques were very useful for interpreting results, future research should explore the use of more complex statistical measures suited for the multivariate and spatial nature of NWP models.
2. Since changing the current Reisner mixed-phase scheme did not produce more accurate results, further investigation could focus on parameterizations that feed into cloud-microphysics such as PBL, soil moisture fluxes, and cloud and clear air radiation.
3. The number of successful snow hits coincident with surface temperatures above freezing provide evidence that allowing snow to exist above freezing is an advantage of using mixed-phase microphysics. However, both Option 5 and 7 tended to prevent snow from adequately melting to rain when snow mixing ratios

were high. Future investigations could focus on putting a high temperature "brake" on the existence of snow at ground level.

4. This study used RAOBs for model verification. Further research could make use of Doppler radar data from Korea (at the time of this research, mainland Japan did not have Department of Defense operated WSR-88D radar sites). The MM5 can provide simulated radar reflectivity of its q_r, $q_{s,}$ and q_g fields. In addition to use of radar, satellite data could also be used in future research because the MM5 can also simulate cloud top temperatures. This would be particularly beneficial in the verification of cloud ice forecasts.
5. The research could be extended to determine whether Option 7, with its higher production of supercooled liquid water, would produce more accurate forecasts of aircraft icing.
6. Finally, since this verification study focused only on East Asia, future research should be extended to other regions of national interest such as Europe or Central Asian theaters.

Appendix A: Geographic and Synoptic Background of Study

Since topography and oceanographic influences have direct impacts on weather and climate, they are critical inputs into the MM5. Therefore, this appendix discusses topographical and oceanographic influences on the East Asian winter weather. With the intended goal of comparing the performance of the two Reisner schemes in forecasting winter precipitation in East Asia, a 20-day case period in January 1998 was selected to represent typical winter regimes for the region. January 1998 was marked by the passage of several extra-tropical systems that resulted in varying amounts of winter precipitation over Japan and Korea.

A.1. Topographical Influences

Osan and Kwang-Ju are located on the Korean Peninsula, the northern portion of which borders China. However, most of Korea is surrounded by water, with the Sea of Japan bordering the east coast and the Yellow Sea bordering the west. Both Osan and Kwang-Ju are located on the western side of the peninsula in an area that consists of coastal plains and low mountains. Osan is situated about 60 km south of Seoul at 37°05'N, 127°02'E. The airfield's elevation is 12 m above sea level (MSL). The Yellow Sea is about 22 km due west, with one inlet to the southwest that comes within 11 km of the base (AFCCC, 2001). Kwang-Ju is located approximately 200 km south of Osan at 35°07'N, 126°49'E. The airfield has an elevation of 13 m (MSL). Kwang-Ju is situated within a region of plains and low mountains with tops below 1,500 m. The base, on the

southwest corner of the peninsula, is approximately 35 km east of the Yellow Sea and 60 km north of the waters of the Korean Straits.

Wajima is a city along the west-central coast of Honshu, the largest of Japan's four main islands. The city is situated on the Noto Peninsula at 37°23'N, 136°54'E; almost entirely surrounded by the Sea of Japan. Wajima's station elevation is 13 m (MSL). The prime reason Wajima was selected as a verification site for this research is the known importance of graupel and riming processes there. Misawa AB is located on northeastern Honshu at 40°42'N, 141°22'E with a station elevation of 33 m (MSL). The base is on the Pacific coast on a very narrow strip of low land between the ocean and the Ou Mountains that run south to north.

A.2. Oceanographic Influences

A major oceanographic influence on sea surface temperatures off East Asia in January is the Kuroshio Current (Thuman, 1991). This warm water current branches off from the North Pacific Equatorial Current in the vicinity of 18° N, 100° E and flows northwestward past Taiwan, Okinawa, and southern Honshu. Near 40°N, off the coast of northern Honshu, the Kuroshio Current converges with a cold-water current, known as the Oyashio Current, which transports cold water from the Bering Sea and the Sea of Okhotsk (Thuman, 1991). This oceanographic convergence zone is responsible for the strong temperature gradient off the coast of northern Honshu (AFCCC, 1997).

Minor currents affecting the Sea of Japan during January are offshoots of the Kuroshio Current and these result in an anti-cyclonic current flow that transports warmer water north along the Honshu coast (AFCCC, 1997). The sea temperature gradient in the

Sea of Japan is strong in the winter varying from a January average of 12°C in the vicinity of the Tsushima Strait to below freezing near the Russian city of Vladivostok. The sea temperature gradient of the Sea of Japan directly accounts for the large amount of lake-effect type snowfall experienced along the west coast of Honshu, including Wajima (Harimaya and Sato, 1991). Post frontal passage, anti-cyclonic flow transports cold and stable Siberian air across the Sea of Japan causing cloud streets over water and snow showers along the Honshu coast as the cold air picks up moisture from the ocean and deposits it inland due to differential surface heating and orographic lift.

The sea temperature gradient is also intense in the Yellow Sea in winter. This gradient is in a ridge pattern with the warm axis closer to the Korean Peninsula and is a consequence of the Kuroshio Counter-Current, which flows from the northern Yellow Sea along the Chinese coast (AFCCC, 1997). To a lesser extent than experienced in the Sea of Japan, the Yellow Sea periodically creates lake effect snow showers inland of the west coast of Korea.

A.3. Synoptic Situation

The case period chosen was typical for the winter season since the Asiatic High is the most dominate surface pressure system over East Asia in winter. The air masses associated with it are extremely cold, which results in a very shallow cold pool depth of below the 850 mb level (AFCCC, 1997). The Asiatic High is usually centered over Mongolia and southern Siberia and has a mean central pressure of 1038 mb. The high has several ridge extensions and the one that mostly influences the winter climate of Korea and Japan extends southeastward toward the Yellow Sea (AFCCC, 1997).

At the same time during the winter months when the Asiatic High is at its greatest extent, the Aleutian Low also reaches its maximum intensity (AFCCC, 1997). The Aleutian Low is a maritime feature situated over the Aleutian Islands in the North Pacific. The mean average central pressure of the low in January is 996 mb. The Aleutian Low in conjunction with the Asiatic High acts to form an intense pressure gradient over East Asia in winter (AFCCC, 1997) and the migratory lows that affected Korea and Japan during the case period tracked northeastward along this storm-track gradient.

The polar jet is most evident over East Asia during the winter months and conditions during this case period were no exception. The position of the polar jet during this period varied between 35° and 45°N latitude. Generally, the subtropical jet flowed northeastward across China merging with the polar jet in the vicinity of Shanghai. The combined jets created a broad band of upper-level winds that often exceeded 200 knots during the study. The trajectory of the migratory lows in this case study followed the polar jet closely.

Yellow Sea, Shanghai, and Taiwan Lows are major winter precipitation producers for Korea and Japan and the case study provides examples of each. Figure A1 depicts a pair of Yellow Sea Lows that influenced the region on 02-03 January 1998. Yellow Sea Lows originally form over Mongolia and track around the southern ridge of the Asiatic High. When the lows reach the relatively warmer temperatures of the Yellow Sea, they intensify bringing strong surface winds and snow showers to the Korean peninsula during late winter (AFCCC, 1997).

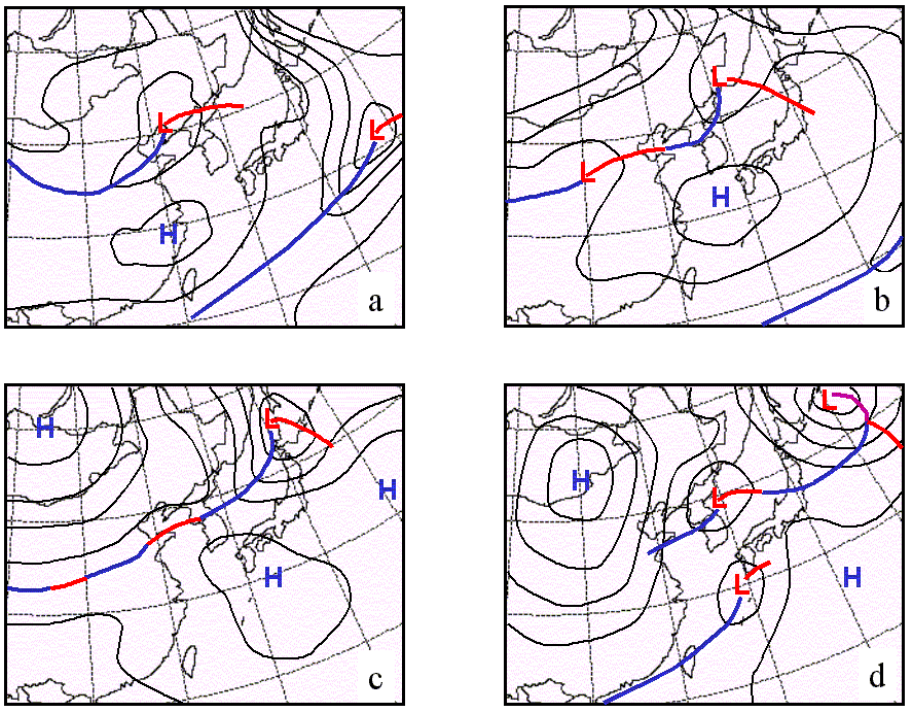

Figure A1. Surface analyses of the synoptic situation of 02-03 January 1998 (a)02/00Z, b) 02/12Z, c) 03/00Z, and d) 03/12Z). These and the following charts were reproduced using archived surface analyses obtained from the National Climatic Data Center, Asheville, NC.

Figure A2 depicts a Shanghai Low that affected the region during the second week of the case study. Shanghai Lows generally form from weakened lows that track eastward off the Tibetan Plateau. As these lows reach the coast of China, they regenerate in strength and move northeastward along the combined sub-tropical and polar jets. Shanghai Lows frequently undergo explosive cyclogenesis off the east coast of Honshu. Explosive cyclogenesis is defined as the deepening of the central sea-level pressure of a low by 12 mb or more during a 12-hour period (Carlson, 1991). Explosive cyclogenesis is primarily a wintertime phenomena and is associated with conditions of extremely strong westerlies and intense sea surface temperature gradients. The intense strength of the combined subtropical/polar jet over Japan in the winter along with the intense sea

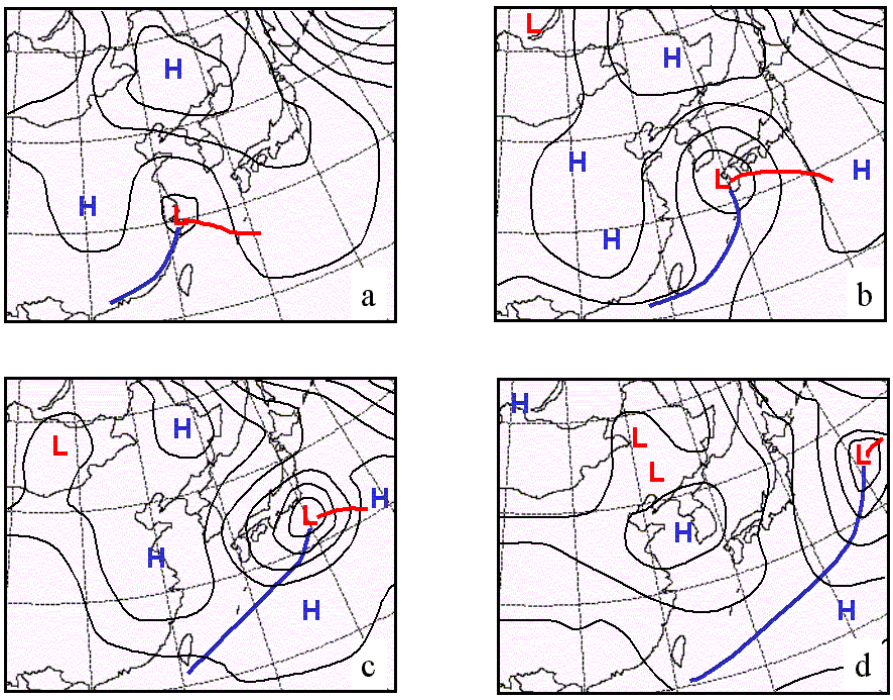

Figure A2. Surface analyses of the synoptic situation of 07-09 January 1998 (a) 07/12Z, b) 08/00Z, c) 08/12Z, and d) 09/00Z).

surface temperature gradient created by the Kuroshio Current provide an ideal environment for explosive cyclogenesis (Carlson, 1991). For this reason, Shanghai Lows can bring massive amounts of snow to Misawa and this particular Shanghai Low resulted in over 30 inches of snowfall for the base.

Figure A3 depicts the third extratropical cyclone type observed during the 20-day study: the Taiwan (or Yangtze) Low. These lows occur during strong cold air outbreaks over China that happen when the center of the Asiatic High moves south of Mongolia. The Taiwan Low originates over the Yangtze River in southern China. When these lows hit the very warm waters of the Taiwan Strait, they undergo rapid cyclogenesis. Taiwan Lows are the most rapid moving of the wintertime East Asian cyclones with speeds averaging 24 knots (Nestor, 1977).

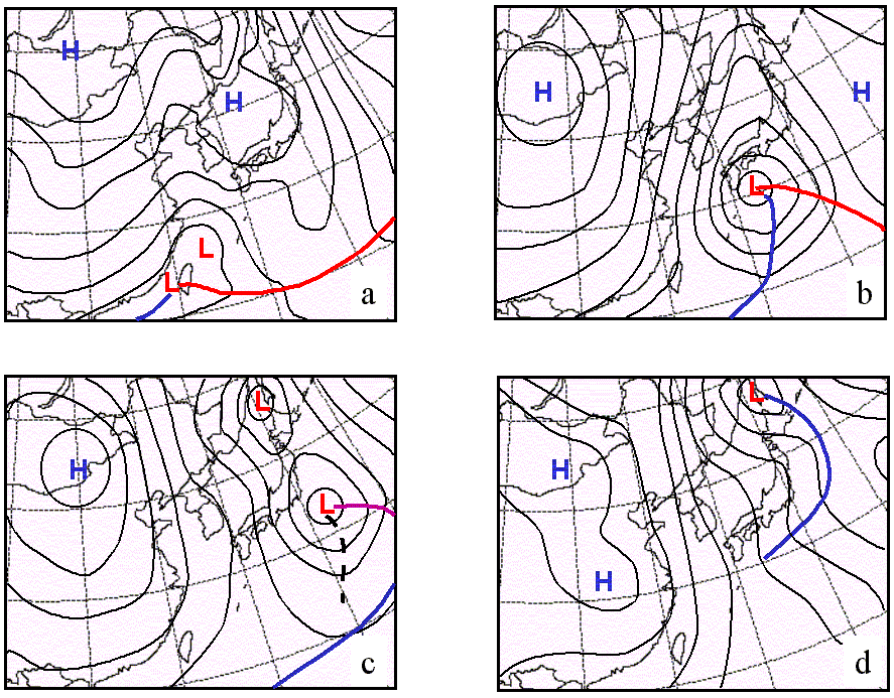

Figure A3. Surface analyses of the synoptic situation of 17-19 January 1998 (a) 17/00Z, b) 18/00Z, c) 18/12Z, and d) 19/00Z).

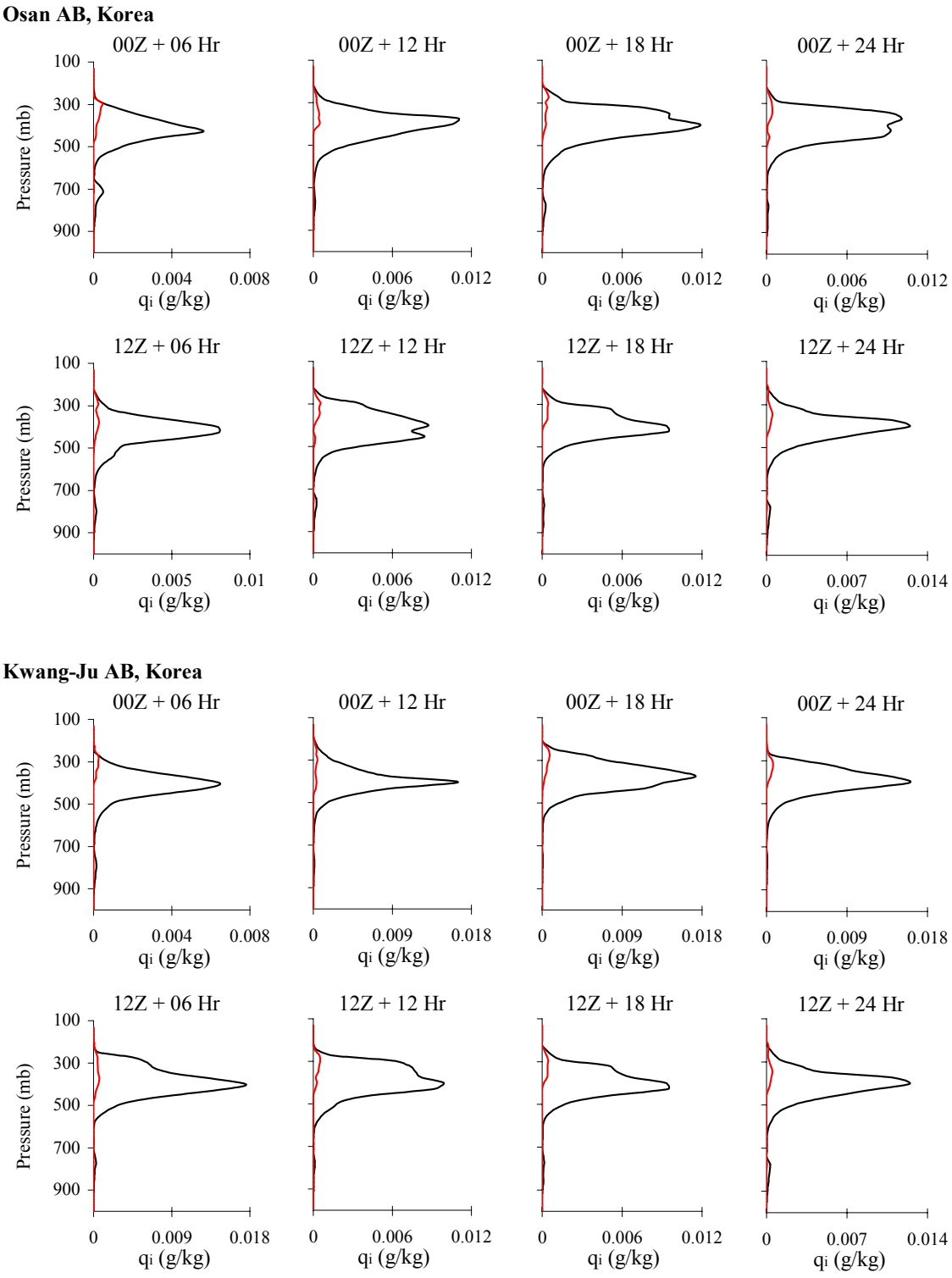

Figure B1. Average MM5 cloud ice for Osan and Kwang-Ju, Korea during period of study. Option 5 is depicted in black and Option 7 is depicted in gray.

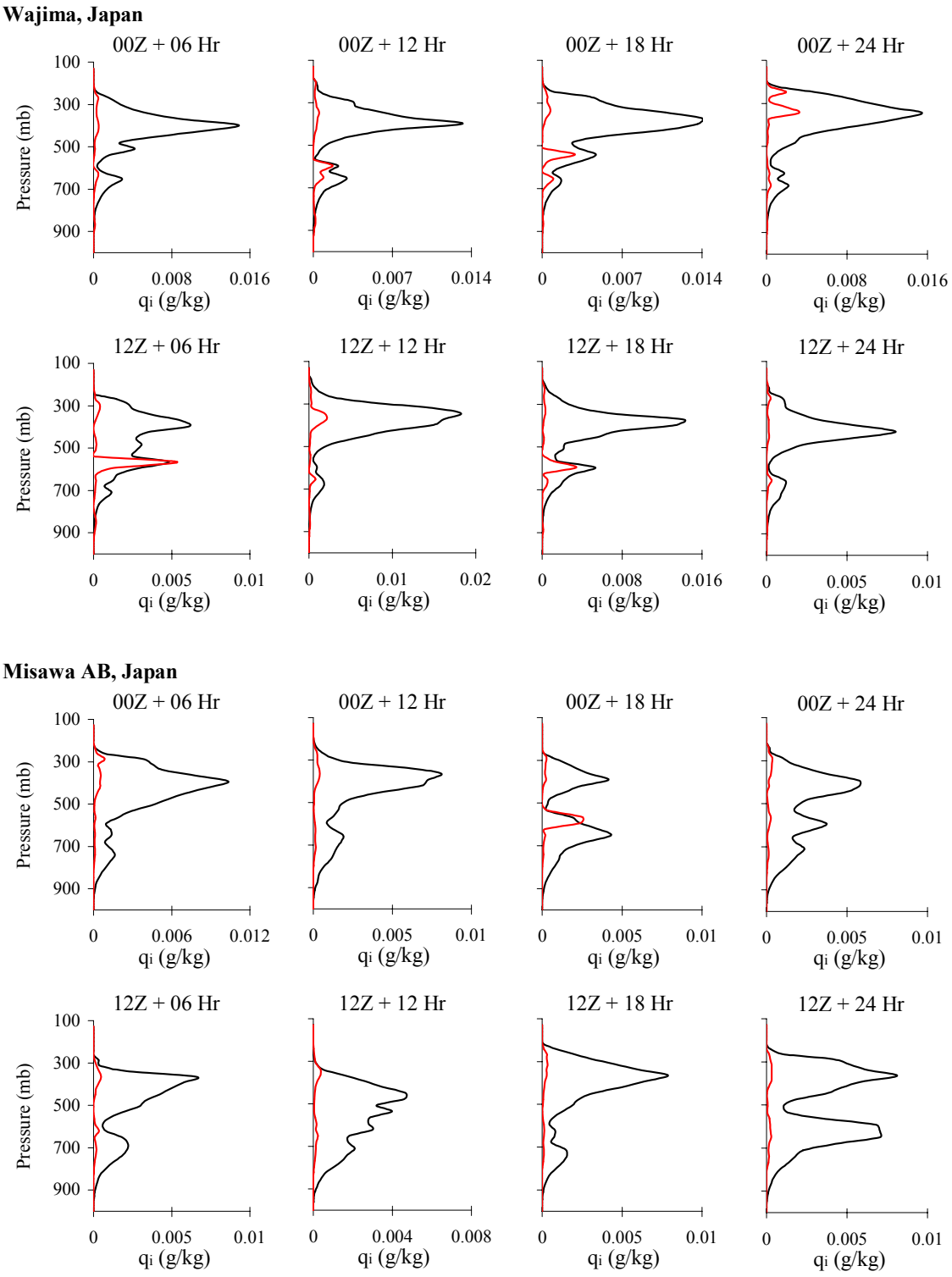

Figure B2. Average MM5 cloud ice for Wajima and Misawa, Japan during period of study. Option 5 is depicted in black and Option 7 is depicted in gray.

Bibliography

Air Force Combat Climatology Center (AFCCC). "Full Year Climatology Narratives". n. pag. http://www.afccc.af.mil. 10 October 2001.

Air Force Weather Agency (AFWA), *Meteorological Techniques*, Technical Note TN-98/002, 1998.

Air Weather Service (AWS) *The Use of the Skew-T, Log P Diagram in Analysis and Forecasting*, Technical Reference (TR) 79-006, 1990.

Barry, Roger G., and Richard J. Chorley, 1968: *Atmosphere, Weather and Climate*, Routledge, 392 pp.

Bernstein, B. C., 2000: Regional and local influences on freezing drizzle, freezing rain, and ice pellet events. *Weather Forecasting*, **15**, 485-508.

Bocchieri, J. R., 1980: The objective use of upper-air soundings to specify precipitation type. *Monthly Weather Review*, **108**, 596-603.

Carbin, G.: "Precipitation Type Algorithms", National Storm Prediction Center, National Centers for Environmental Prediction. n. pag. http://www.spc.noaa.gov/staff/carbin/nwa99. 05 December 2001.

Carlson, T. N., 1991: *Mid-latitude Weather Systems*, Routledge, 507 pp.

Colle, B. A., K. J. Westrick, and C.F. Mass, 1999: Evaluation of MM5 and Eta-10 precipitation forecasts over the Pacific Northwest during the cool season. *Weather Forecasting*, **14**, 137-154.

Cooperative Program for Operational Meteorology Education and Training (COMET). "How Models Produce Clouds and Precipitation", University Corporation for Atmospheric Research. n. pag. http://www.comet.ucar.edu. 26 January 2002.

Dudhia, J., D. Gill, Y-R Guo, K.W. Manning, and W. Wang, 2001: PSU/NCAR Mesoscale Modeling System Tutorial Class Notes and User's Guide: MM5 Modeling System Version 3, National Center for Atmospheric Research, 170 pp.

Grell, G. A., J. Dudhia, and D.R. Stauffer, 1994: *A Description of the Fifth Generation Penn State/NCAR Mesoscale Model (MM5), NCAR Tech Note 398*, National Center for Atmospheric Research, 117 pp.

Harimaya, T, and M. Sato, 1991: The riming proportion in snow particles falling on coastal areas. *Journal of the Meteorological Society of Japan*, **70**, 57-64.

Hamill, T. M., 1998: Hypothesis tests for evaluating numerical precipitation forecasts. *Weather and Forecasting*, **14**, 155-167.

Manning, K. W., and C. A. Davis, 1997: Verification and sensitivity experiments for the WISP94 MM5 forecasts. *Weather and Forecasting*, **12**, 719-735.

Meteorology and Training (MetEd). "Characteristics of Operational NWP Models", National Oceanic and Atmospheric Administration. n. pag. http://meted.ucar.edu/. 26 January 2002.

Naval Environmental Prediction Research Facility, *The Environment of South Korea and Adjacent Sea Areas,* NAVENVPREDRSCHFAC Technical Note 77-03, 1977

Panofsky, H.A., and G.W. Brier, 1968: *Some Applications of Statistics to Meteorology*, Pennsylvania State University Press, 224 pp.

Rasmussen, R. M., and W. A. Cooper, 1993: *Winter Icing and Storms Project 1994 (WISP94) Scientific Overview*, National Center for Atmospheric Research, 46 pp.

Reisner, J., R. M. Rasmussen, R. T. Bruintjes, 1997: Explicit forecasting of supercooled liquid water in winter storms using the MM5 mesoscale model. *Quarterly Journal of the Royal Meteorological Society*, **124**, 1071-1107.

Rogers, R.R., and M.K. Yau, 1989: *A Short Course in Cloud Physics*, Pergamon Press, 293 pp.

Rutledge, S.A., and P.V. Hobbs, 1984: The mesoscale and microscale structure and organization of clouds and precipitation in midlatitude cyclones. XII: A diagnostic modeling study of precipitation development in narrow cold-frontal rainbands. *Journal of the Atmospheric Sciences*, **41**, 2949-2972.

Stanski, H. R., L. J. Wilson, and W. R. Burrows, 1989: Survey of common verification methods in meteorology. World Meteorological Organization Technical Document 358, 114 pp.

Stewart, R.E., 1985: Precipitation types in winter storms. *Pure Applied Geophysics*, **123**, 597-609.

_____, and P. King, 1986: Freezing precipitation in winter storms. *Monthly Weather Review*, **115**, 1270-1279.

Stoelinga, M. T., 2000: *A User's Guide to RIP Version 3: A Program for Visualizing PSU/NCAR Mesoscale Model System Output*, University of Washington, 62 pp.

Sun Tzu, 6th century B.C: *The Art of War*, Delacorte Press, 82 pp.

Thurman, H. V., 1991: *Introductory Oceanography*, Macmillan Publishing Company, 526 pp.

Wallace, J.M., and P.V. Hobbs, 1977: *Atmospheric Science: An Introductory Survey*, Academic Press, 467 pp.

Zerr, R.J., 1997: Freezing rain - an observational and theoretical study. *Journal of Applied Meteorology*, **36**, 1647-1661.

Vita

Captain Dean J. Carter enlisted in the U.S. Air Force in May 1987. After attending weather technical training at Chanute AFB, Illinois, his first operational assignment was at Hurlburt Field, Florida as a radiosonde operator. He served in subsequent assignments at Kunsan AB, South Korea and R.A.F. Alconbury, United Kingdom as a weather specialist. In December 1992, at the rank of Staff Sergeant, he was awarded an AFROTC scholarship in the field meteorology and was discharged from active duty.

In December 1995, Captain Carter was commissioned through the Detachment 595 AFROTC at North Carolina State University where he was recognized as a Distinguished Graduate and nominated for a regular commission. His first assignment as a commissioned officer was to the 49th Operational Support Squadron at Holloman AFB, New Mexico as a wing weather officer in January 1996. While assigned at Holloman, he deployed to Al Jaber AB, Kuwait in support of Operation Desert Strike in September, 1996. In July 1997, he was assigned to Headquarters Fifth Air Force at Yokota AB, Japan as a staff weather officer and contingency planner. While stationed at Yokota, Captain Carter deployed to Vicenza, Italy in support of Operation Deliberate Forge. In September 2000, he entered the Graduate School of Engineering and Management at the Air Force Institute of Technology. Upon graduation, he will be assigned to the 26th Operational Weather Squadron at Barksdale AFB, Louisiana.

REPORT DOCUMENTATION PAGE	Form Approved OMB No. 0704-0188

PLEASE DO NOT RETURN YOUR FORM TO THE ABOVE ADDRESS.

1. REPORT DATE *(DD-MM-YYYY)*	2. REPORT TYPE	3. DATES COVERED *(From - To)*
14-01-2002	Master's Thesis	Sep 2000 - Jan 2002

4. TITLE AND SUBTITLE

VERIFICATION OF MM5 CLOUD MICROPHYSICS SCHEMES FOR EAST ASIA

5a. CONTRACT NUMBER

5b. GRANT NUMBER

5c. PROGRAM ELEMENT NUMBER

6. AUTHOR(S)

Carter, Dean, J., Captain, USAF

5d. PROJECT NUMBER

5e. TASK NUMBER

5f. WORK UNIT NUMBER

7. PERFORMING ORGANIZATION NAME(S) AND ADDRESS(ES)

Air Force Institute of Technology
Graduate School of Engineering and Management (AFIT/EN)
2950 P Street, Building 640
WPAFB OH 45433-7765

8. PERFORMING ORGANIZATION REPORT NUMBER

AFIT/GM/ENP/02M-01

9. SPONSORING/MONITORING AGENCY NAME(S) AND ADDRESS(ES)

PACAF/DOWO
Atten: Mr. John Feckter
25E St., Ste I232
Hickam AFB, Hawaii 96853
DSN: 315-448-1533

AFWA/DNXM
106 Peacekeeper Dr.
Offutt AFB, NE 68113-4039
DSN: 271-3893

10. SPONSOR/MONITOR'S ACRONYM(S)

11. SPONSOR/MONITOR'S REPORT NUMBER(S)

12. DISTRIBUTION/AVAILABILITY STATEMENT

APPROVED FOR PUBLIC RELEASE; DISTRIBUTION UNLIMITED

13. SUPPLEMENTARY NOTES

14. ABSTRACT

This research compares biases of the Reisner Mixed-Phase Explicit Moisture Microphysics graupel and non-graupel schemes to determine if including graupel and riming processes within the Fifth Generation Mesoscale Model (MM5) will lead to improved forecasts of winter precipitation for Korea and Japan. MM5 forecasts were generated every 12 hours for a 20-day case period from January 1998. Model derived meteorological fields were interpolated to the station coordinates of four verification sites within the East Asian domain and radiosonde observations were used to compare the differences between the average temperature and water vapor errors of the two cloud microphysics schemes. Analysis of the results shows significant differences between the schemes in the magnitude of humidity errors within the lower atmosphere of the model and provides evidence that the more complicated graupel and riming scheme will not increase the skill of the MM5 in forecasting winter precipitation for Japan and Korea. The underlying conclusion of this research is that AFWA should not alter the cloud microphysics scheme currently employed to determine winter precipitation type for its East Asian forecast window.

15. SUBJECT TERMS

Winter Precipitation, Fifth Generation Mesoscale (MM5), Reisner Mixed-Phase Microphysics, Graupel and Riming Processes

16. SECURITY CLASSIFICATION OF:			17. LIMITATION OF ABSTRACT	18. NUMBER OF PAGES	19a. NAME OF RESPONSIBLE PERSON
a. REPORT	b. ABSTRACT	c. THIS PAGE			Lt Col Ronald P. Lowther
U	U	U	UU	88	19b. TELEPHONE NUMBER *(Include area code)* (937) 255-3636, ext 4645